Light Dark World 2025

Detecting Ultralight Dark Matter with Matter Effect

Speaker: Xucheng Gan

DESY, Hamburg

2504.11522

Collaborators:

Da Liu, Di Liu, Xuheng Luo, Bingrong Yu

To Fit Cosmology Session…

Millicharged Relics Reveal Massless Dark Photons,
2211.05139, Berlin, Dror, XG, Ruderman

Cosmologically varying kinetic mixing,
2302.03056, XG, Liu

Cosmic millicharge background and reheating probes
2308.07951, XG, Tsai

Shaping dark photon spectral distortions
2409.12940, Arsenadze, Caputo, XG, Liu, Ruderman

Dark Matter Landscape

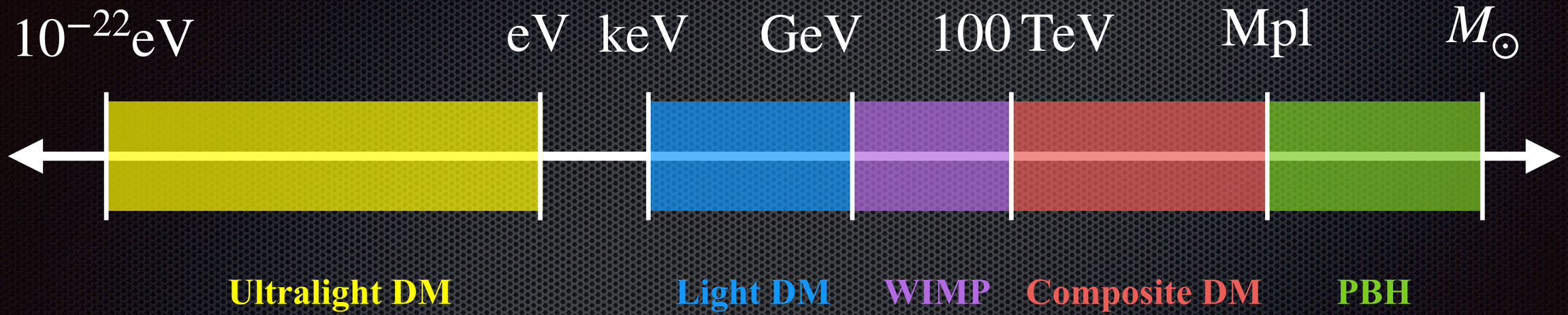

Ultralight DM

Classical behaviors → Interesting Phenomena

Quadratic Coupling

$$\frac{1}{\Lambda^2}\phi^2\mathcal{O}_{\rm SM} \to F^2,\ G^2,\ m_f\bar{f}f$$

$$\mathbb{Z}_2:\ \phi \to -\phi$$

Axion

Hook et al. 2017, Kim et al. 2023,
Beadle et al. 2023, …

Dilaton

Damour et al. 1992,
Sibiryakov et al. 2020, …

Other Scalars

Brzeminski et al. 2020,
Gan et al. 2023, …

Quadratic Coupling

Benchmark Model

$$\frac{1}{\Lambda^2}\phi^2\mathcal{O}_{\rm SM} \to F^2,\ G^2,\ m_f\bar{f}f$$

$$\mathbb{Z}_2:\ \phi \to -\phi$$

Ordinary Matter

$$\mathcal{O}_{\rm SM} \to \langle\mathcal{O}_{\rm SM}\rangle$$

Effective Mass

$$m_{\rm M}^2 \sim \frac{\langle\mathcal{O}_{\rm SM}\rangle}{\Lambda^2}$$

Matter Effect

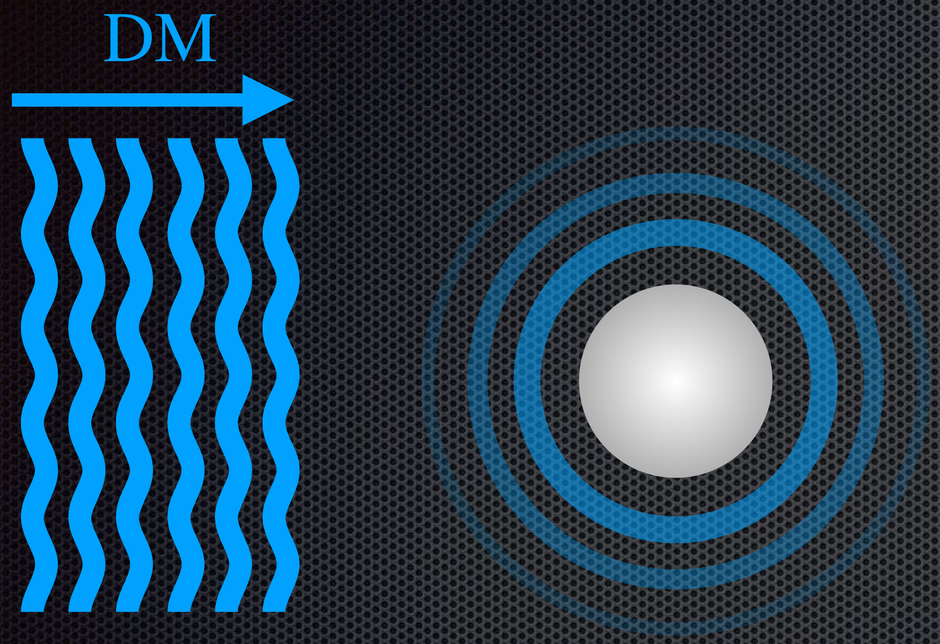

Ordinary Matter

$$\mathcal{O}_{\rm SM} \to \langle \mathcal{O}_{\rm SM} \rangle$$

Effective Mass

$$m_{\rm M}^2 \sim \frac{\langle \mathcal{O}_{\rm SM} \rangle}{\Lambda^2}$$

Matter Effect

Ordinary Matter

Scattering Force

Background-Induced Force

$\mathcal{O}_{\rm SM} \to \langle \mathcal{O}_{\rm SM} \rangle$

Effective Mass

$$m_{\rm M}^2 \sim \frac{\langle \mathcal{O}_{\rm SM} \rangle}{\Lambda^2}$$

Scattering Force

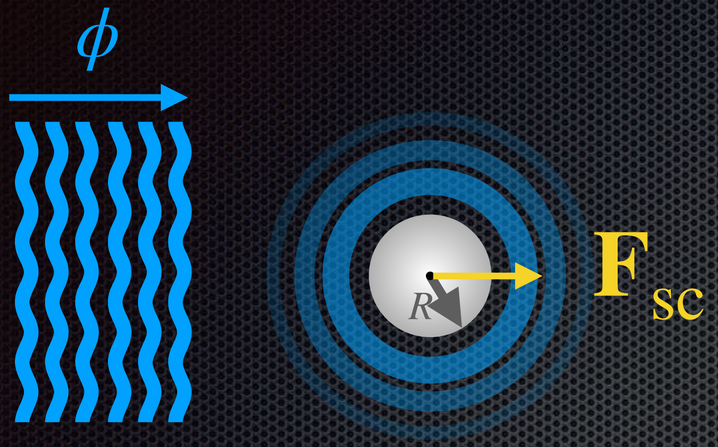

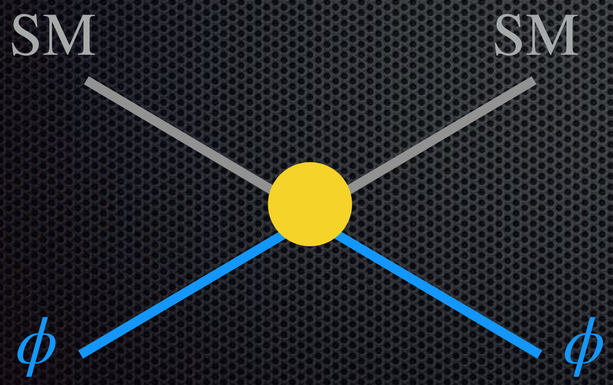

Scattering Force

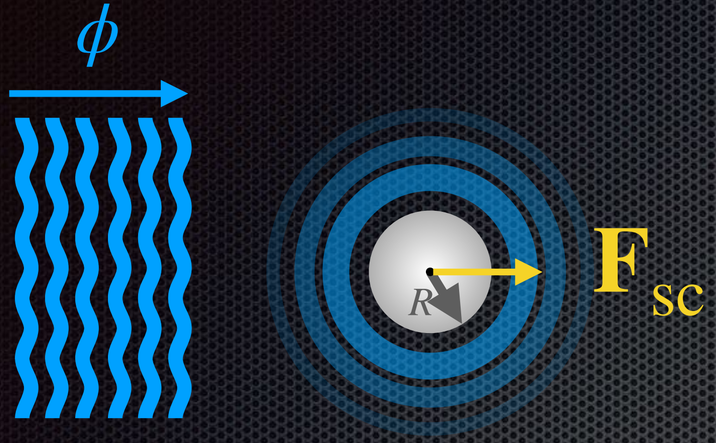

$$\sigma_{\rm T} \sim \frac{(m_{\rm M}^2 V_R)^2}{4\pi}$$ Coherent Scattering

$$\mathbf{F}_{\rm sc} \sim \sigma_{\rm T} \times \rho_\phi v_\phi^2 \times \hat{k}$$

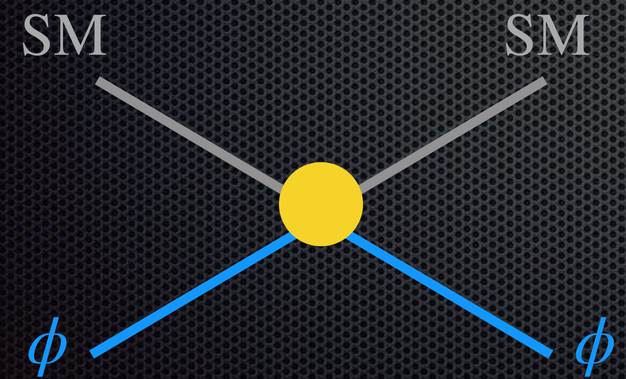

$$a \sim 10^{-13}\,\mathrm{m/s^2} \times \left(\frac{1\mathrm{cm}}{R}\right) \times (m_{\rm M} R)^4$$

Also see Day, Liu, Luty, and Zhao 2023

Background-Induced Force

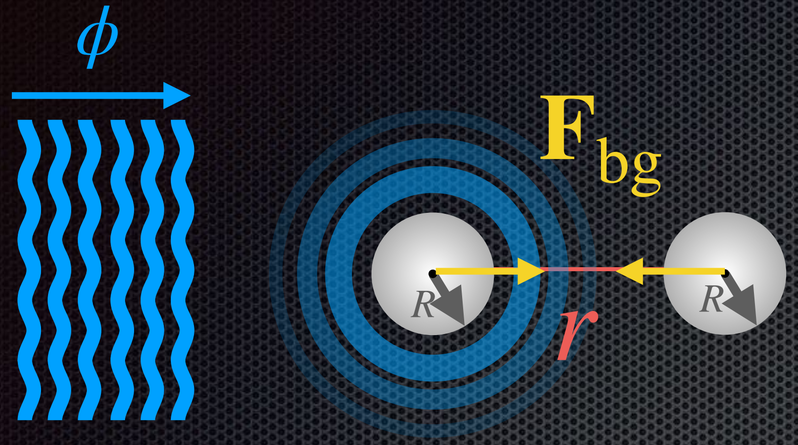

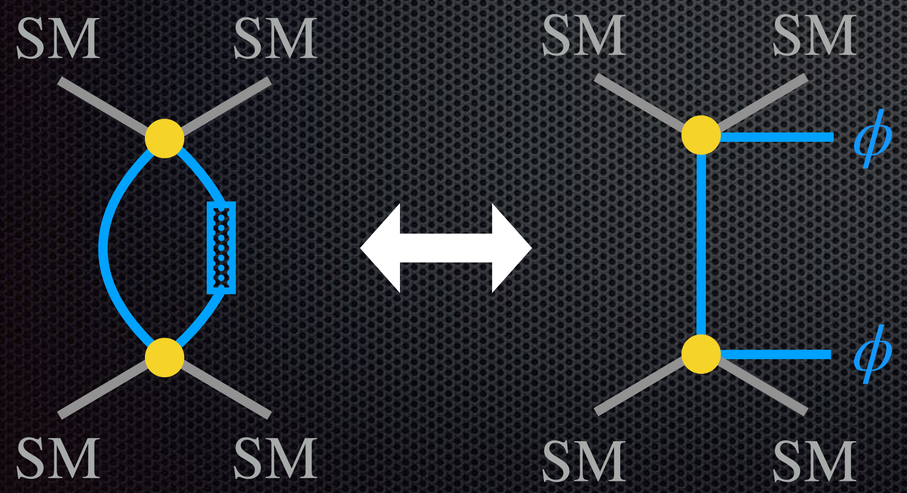

Background-Induced Force

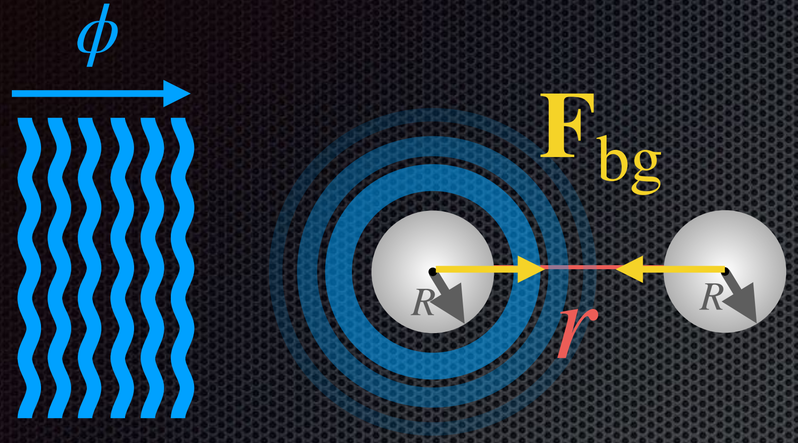

$$\mathbf{F}_{\rm bg} \sim \frac{\rho_\phi}{m_\phi^2} \; (m^2_{\mathrm{M},\mathcal{S}} V_{R,\mathcal{S}}) \; (m^2_{\mathrm{M},\mathcal{T}} V_{R,\mathcal{T}}) \; \frac{1}{r^2}$$

ϕ^2	Source Mass Coherence	Test Mass Coherence	Inverse Square

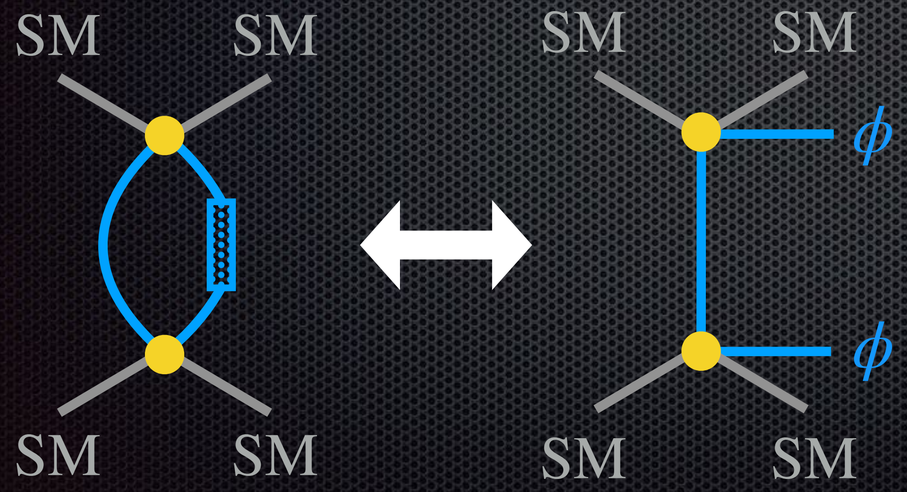

$$a \sim 10^{-13}\,\mathrm{m/s^2} \times \left(\frac{1\mathrm{cm}}{R}\right) \times \frac{(m_{\rm M} R)^4}{(k_\phi r)^2}$$

$\mathbf{F}_{sc}$ vs $\mathbf{F}_{bg}$

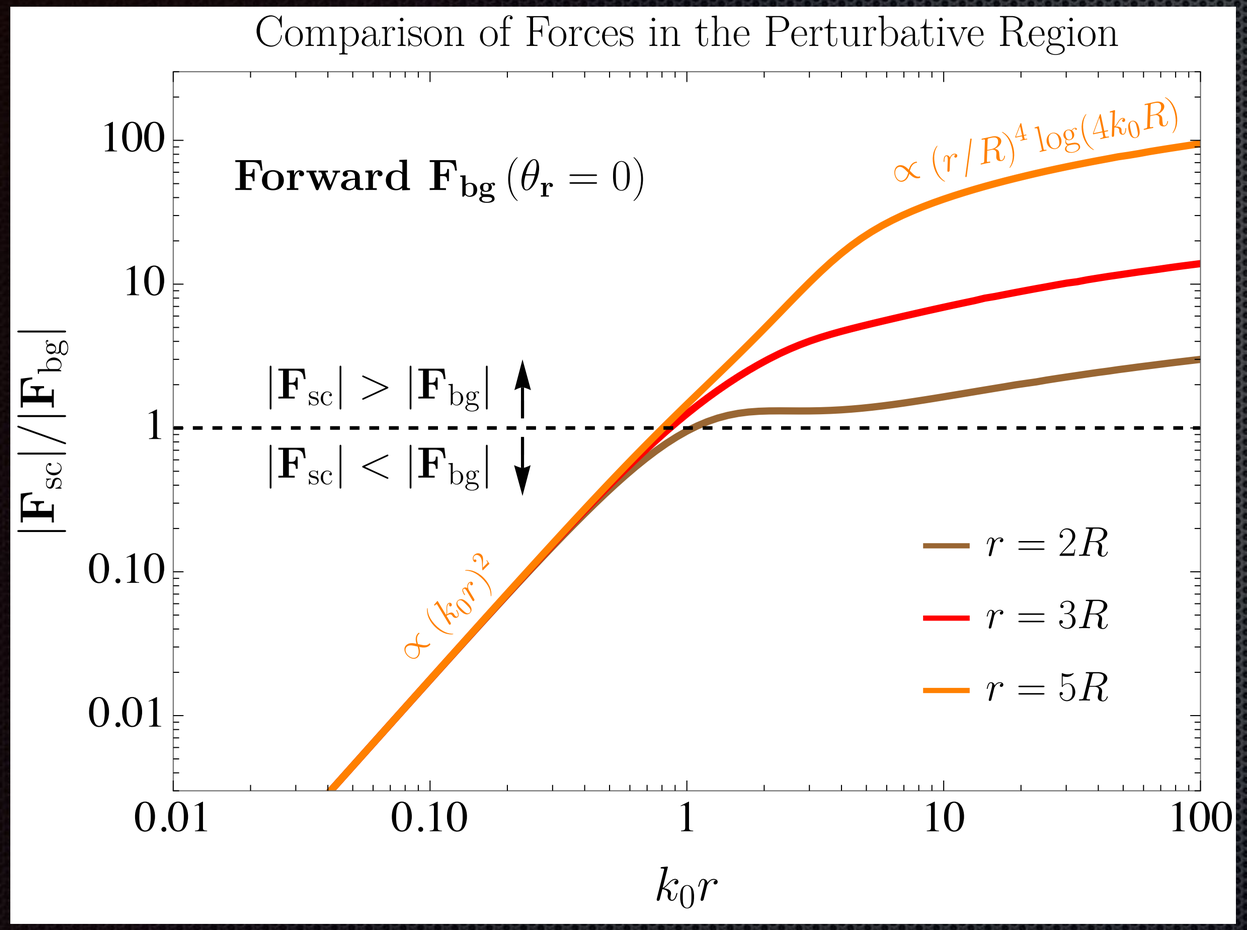

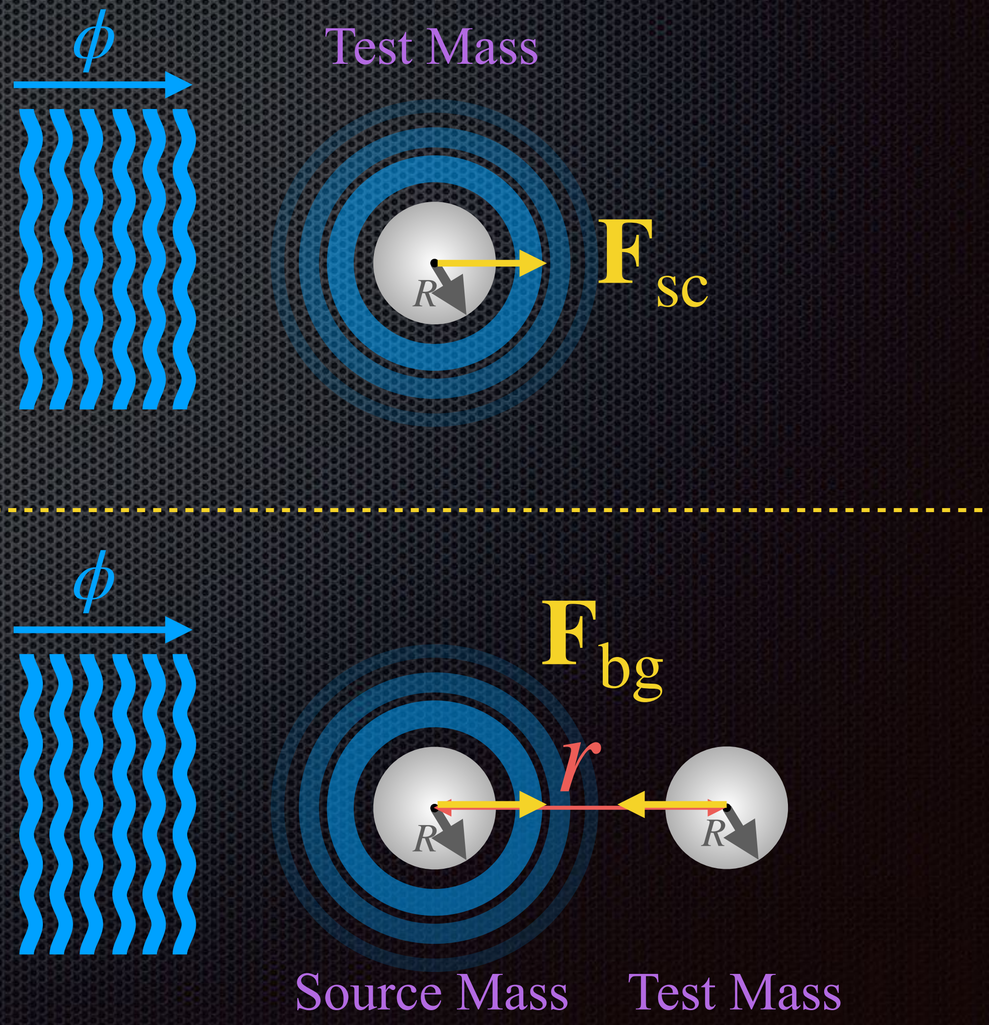

Unified Treatment

$$\mathbf{F}_{\rm sc} \sim \frac{(m_{\rm M}^2 V_R)^2}{4\pi} \times \rho_\phi v_\phi^2 \times \text{Form Factor}$$

$$\mathbf{F}_{\rm bg} \sim \frac{\rho_\phi}{m_\phi^2} (m_{{\rm M},\mathcal{S}}^2 V_{R,\mathcal{S}})(m_{{\rm M},\mathcal{T}}^2 V_{R,\mathcal{T}}) \frac{1}{r^2} \times \text{Form Factor}$$

Unified Treatment

$$\mathbf{F}_{\rm sc} \sim \frac{(m_{\rm M}^2 V_R)^2}{4\pi} \times \rho_\phi v_\phi^2 \times \text{Form Factor}$$

$$\mathbf{F}_{\rm bg} \sim \frac{\rho_\phi}{m_\phi^2} (m_{{\rm M},\mathcal{S}}^2 V_{R,\mathcal{S}})(m_{{\rm M},\mathcal{T}}^2 V_{R,\mathcal{T}}) \frac{1}{r^2} \times \text{Form Factor}$$

Field Oscillation+Finite Phase Space+Finite Geometry

Decoherence, Screening, Descreening

Classification

k_0: Incident Momentum

m_{M}: Effective Mass

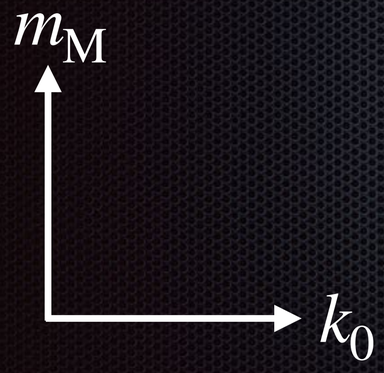

Classification

$m_{\mathrm{M}} = k_0$

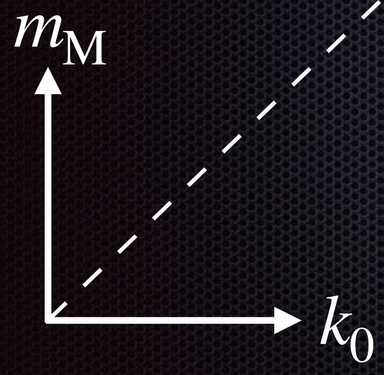

k_0: Incident Momentum

m_{M}: Effective Mass

Classification

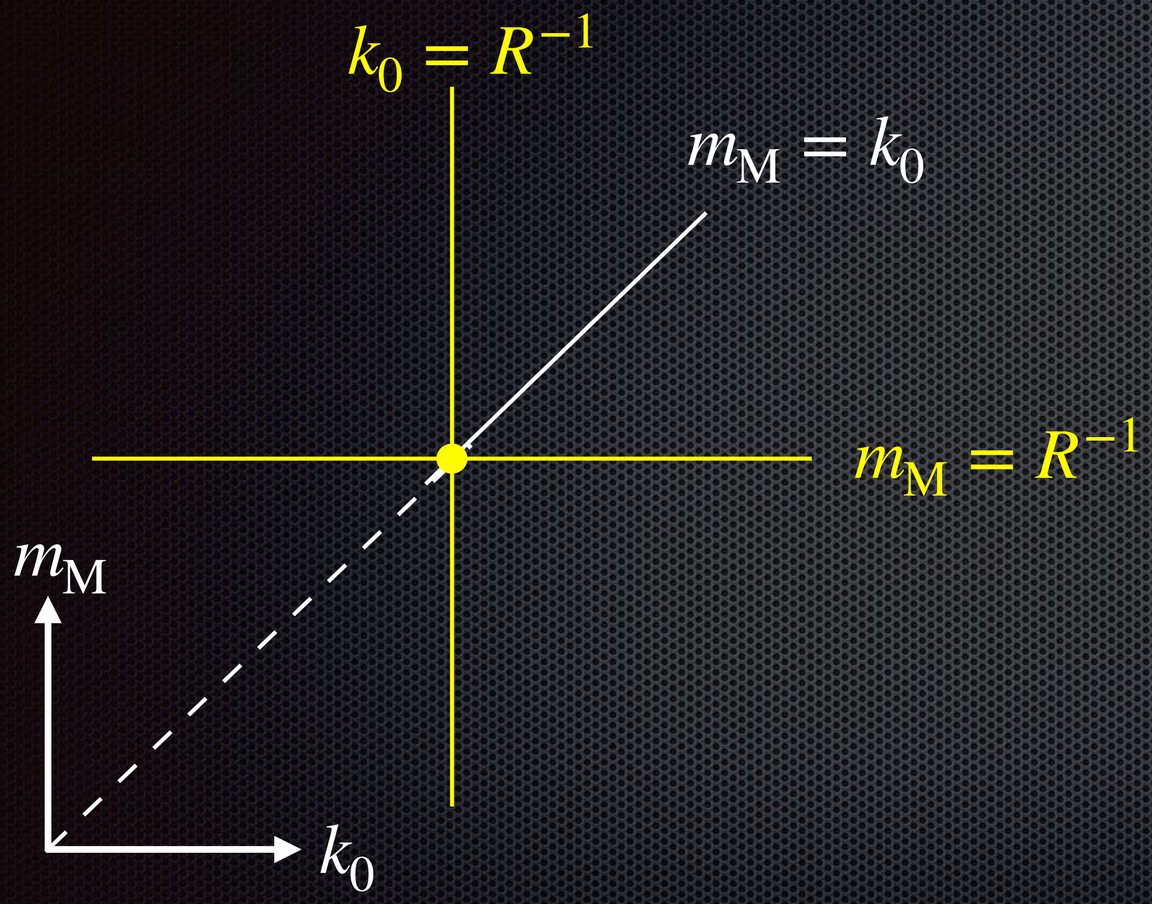

k_0: Incident Momentum

m_{M}: Effective Mass

R: Radius of Scattered Sphere

Classification

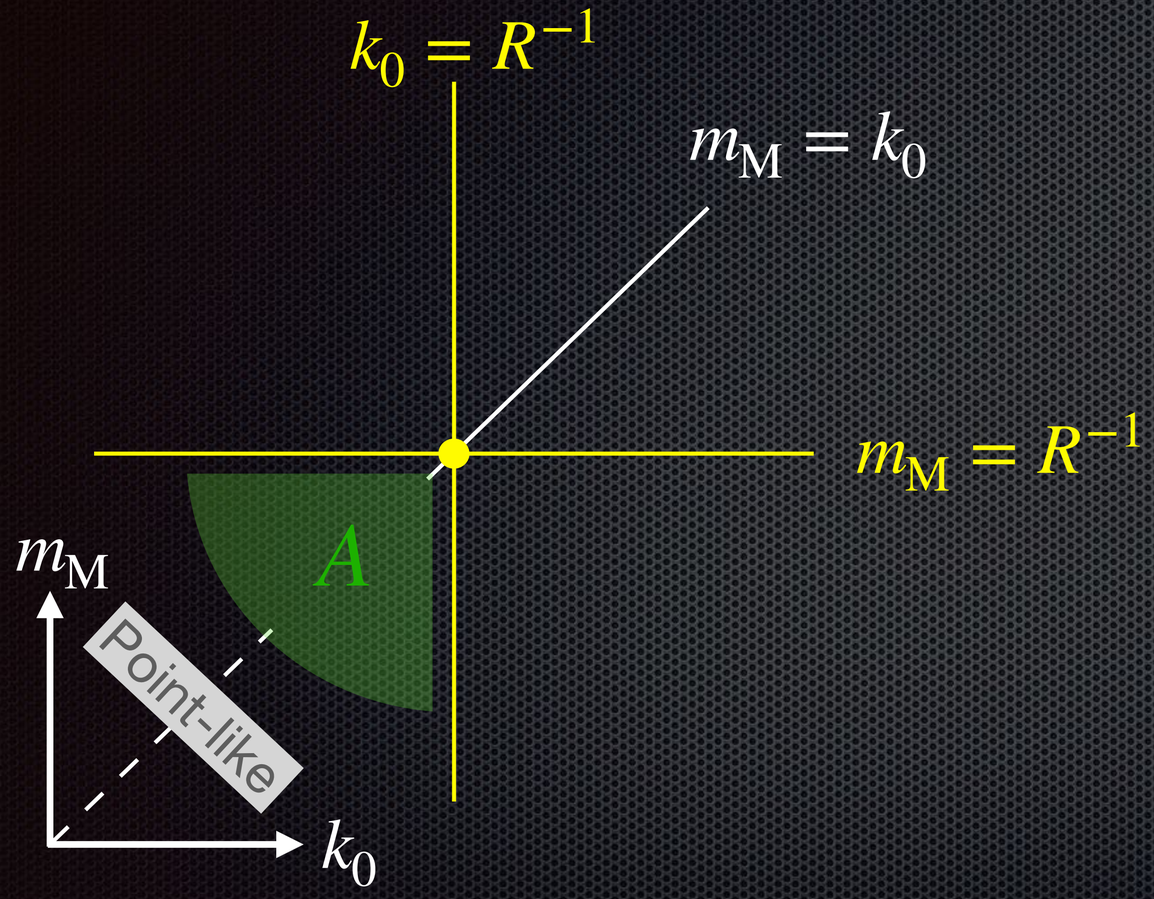

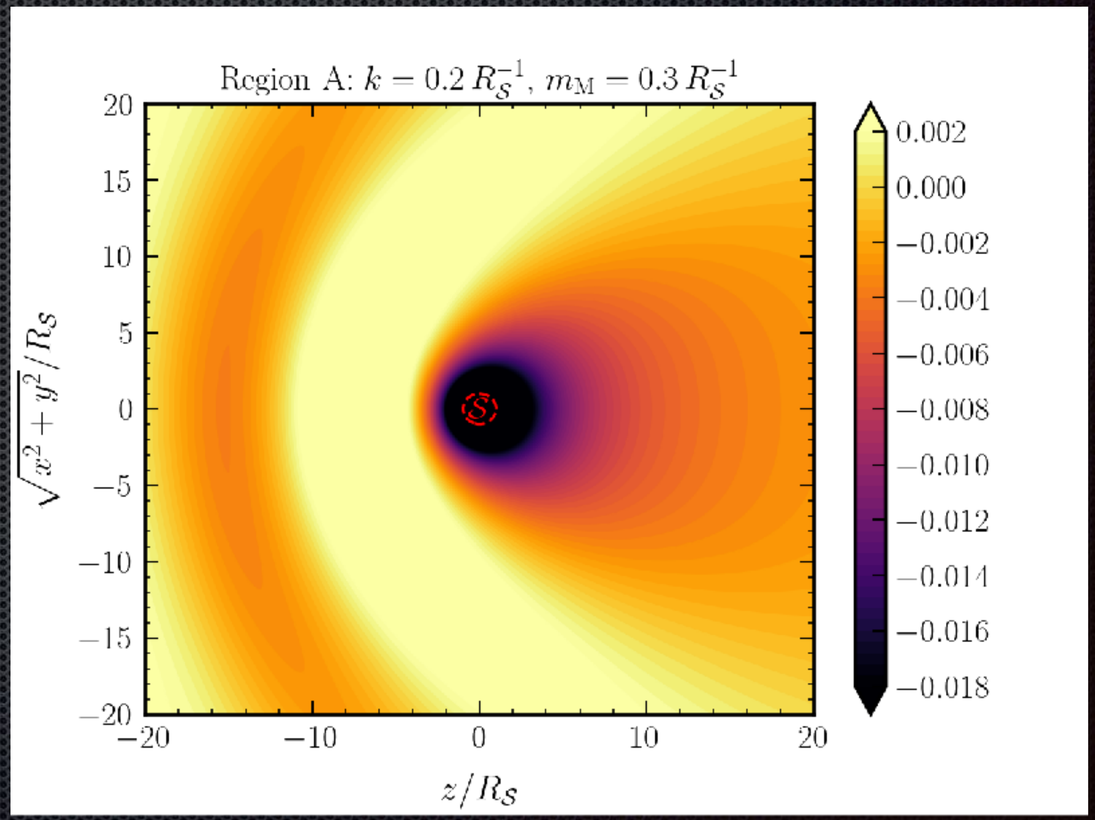

s-wave: oscillatory when $kr > 1$

Classification

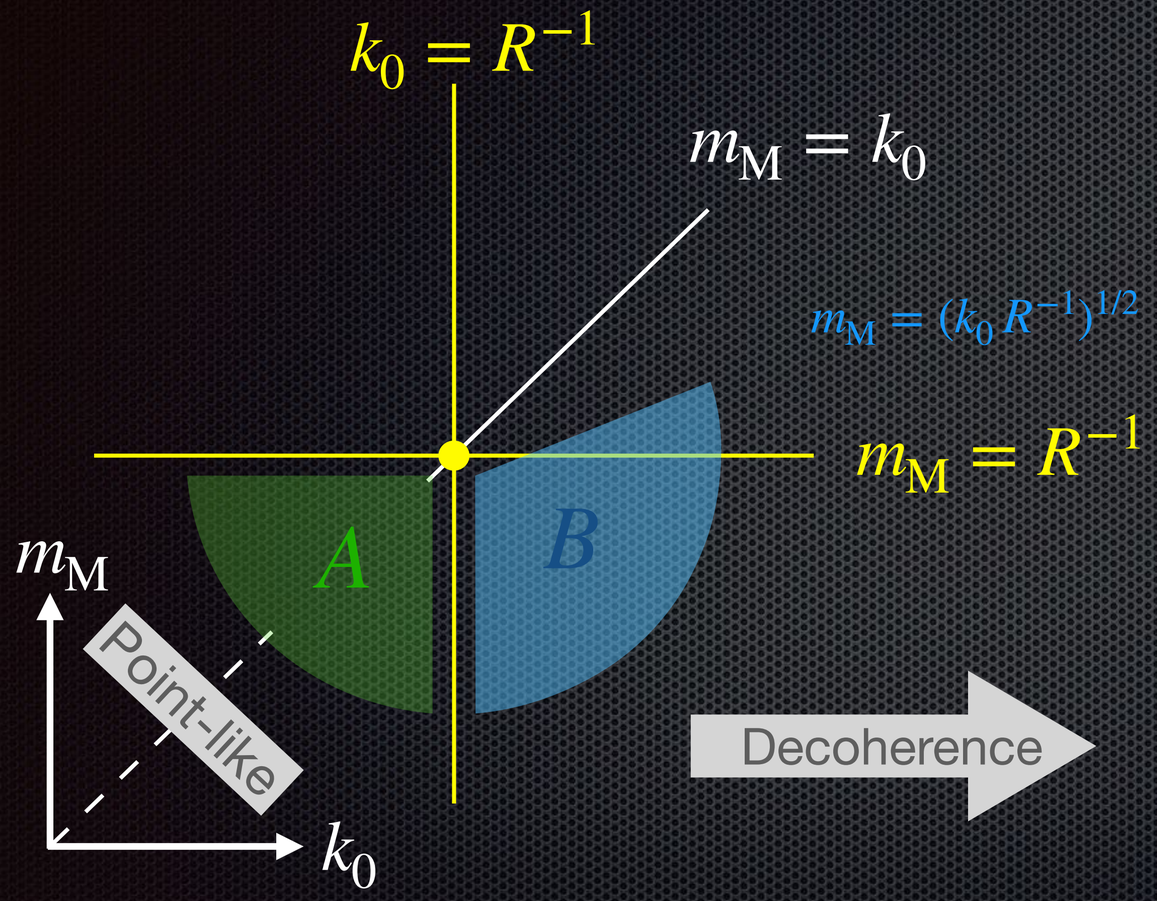

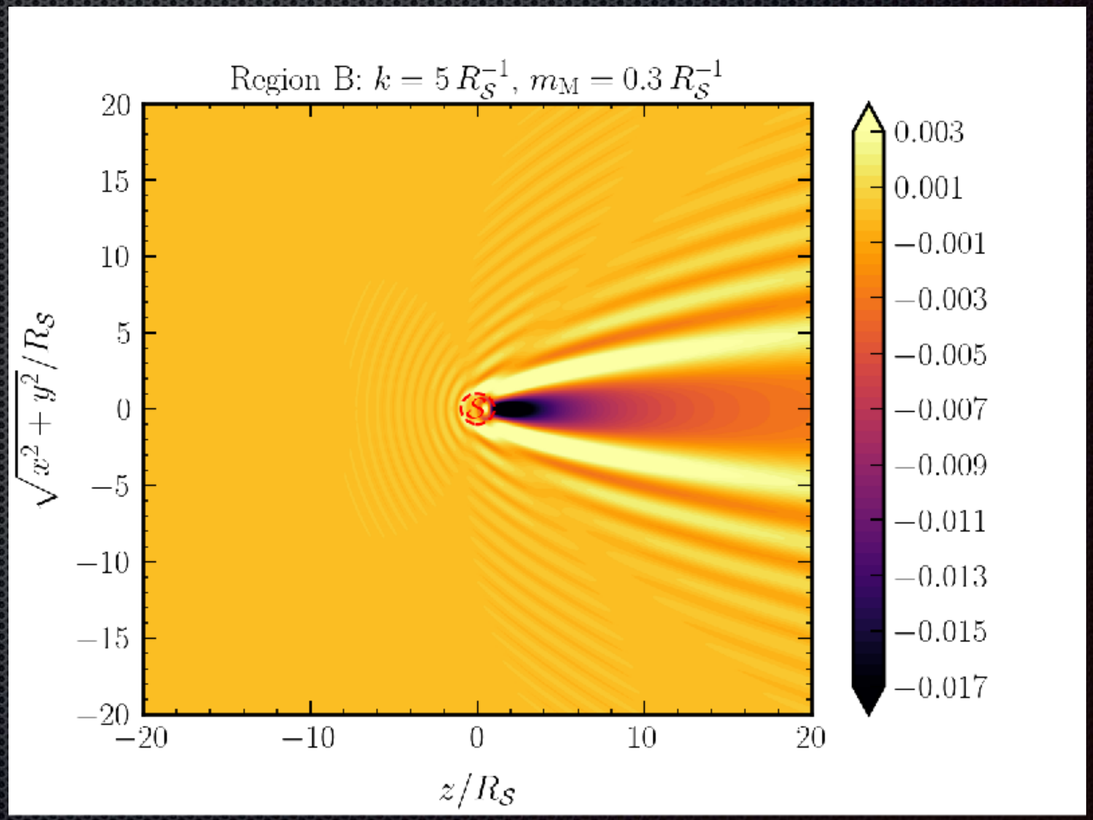

Classification

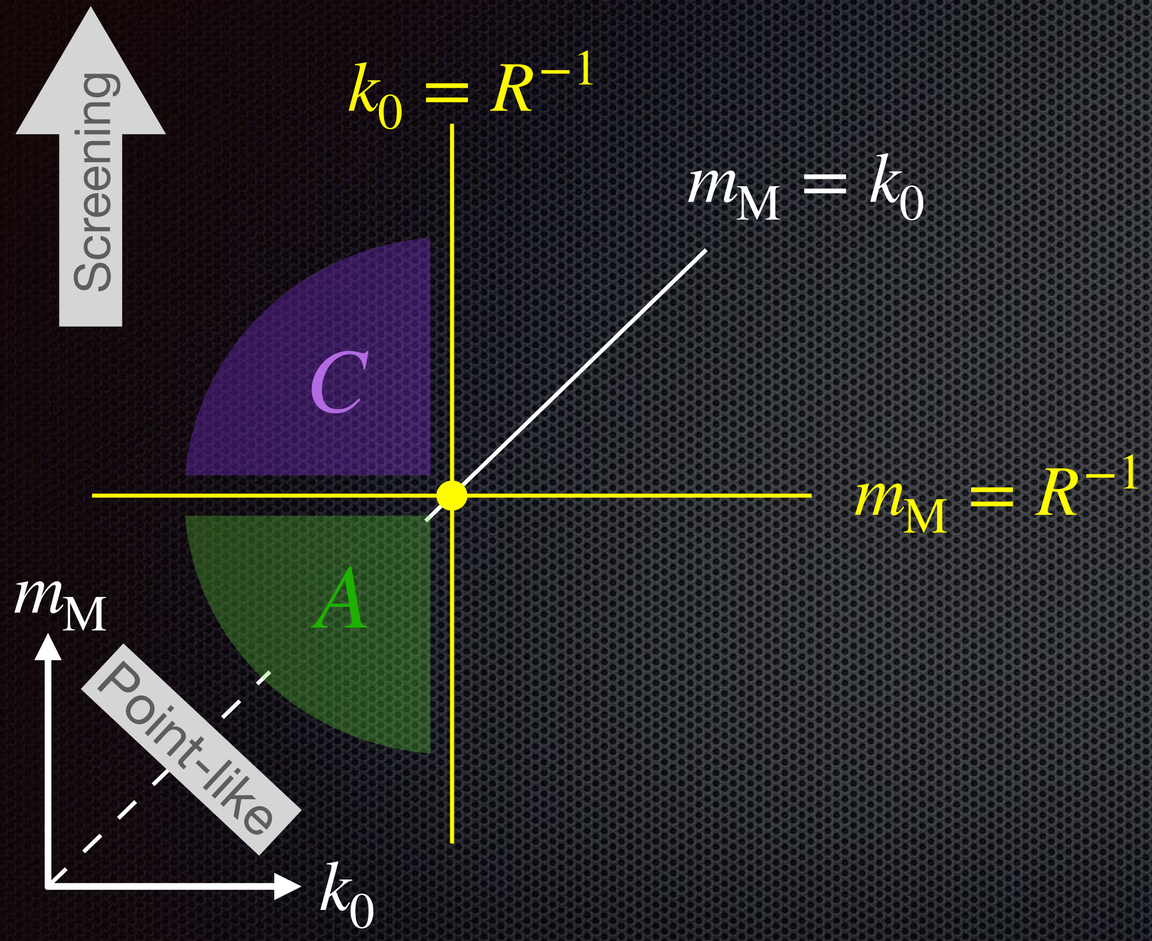

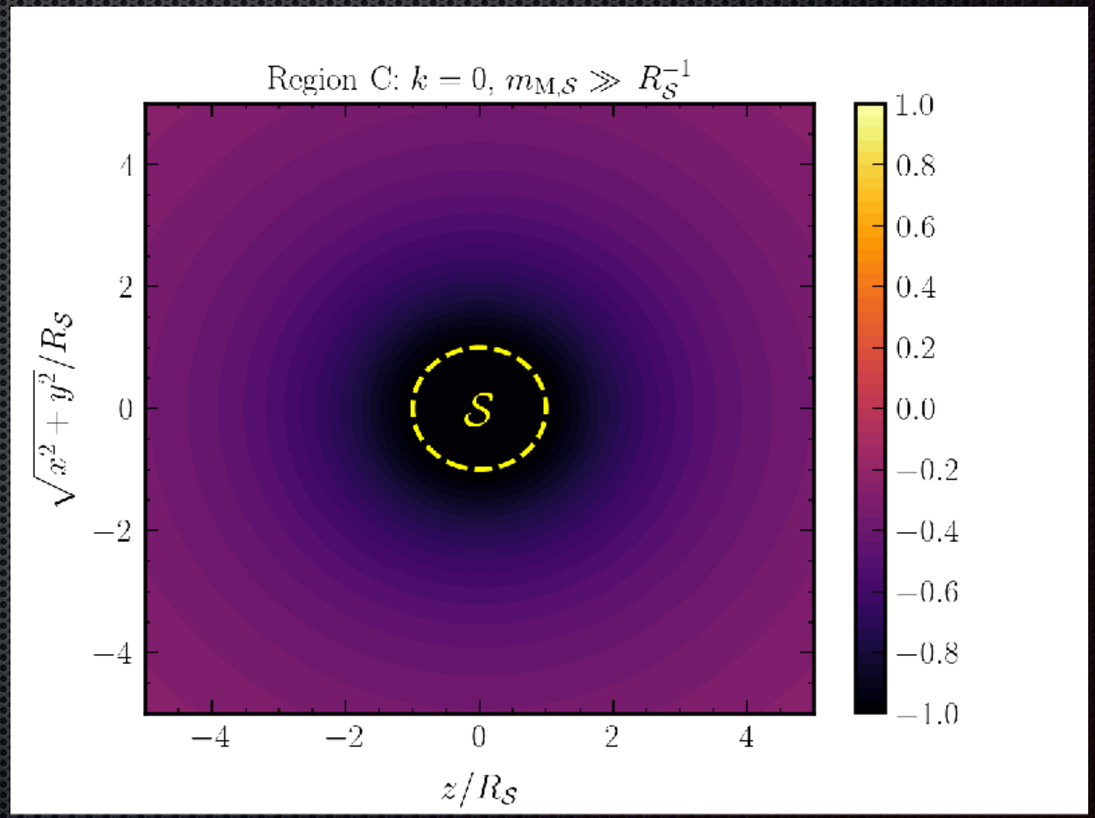

Classification

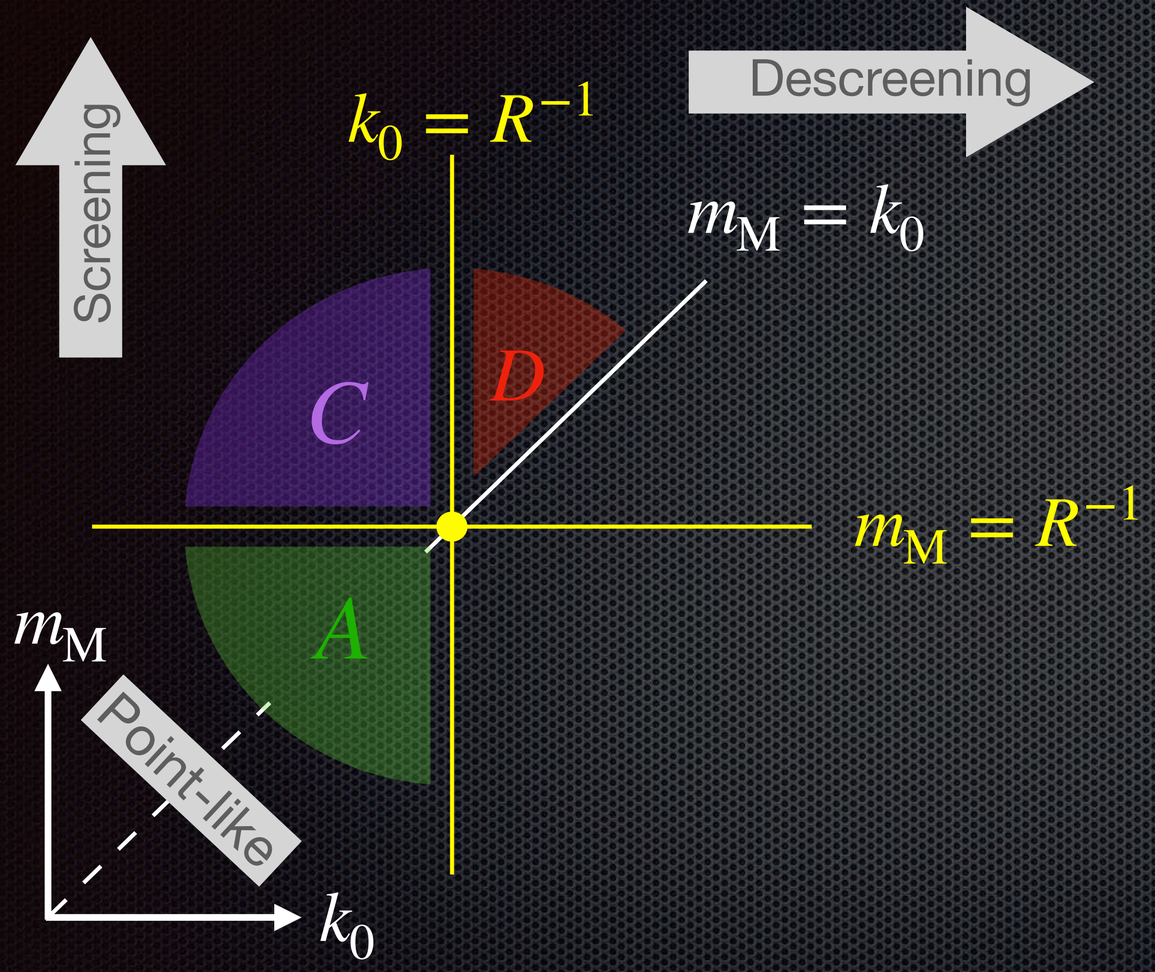

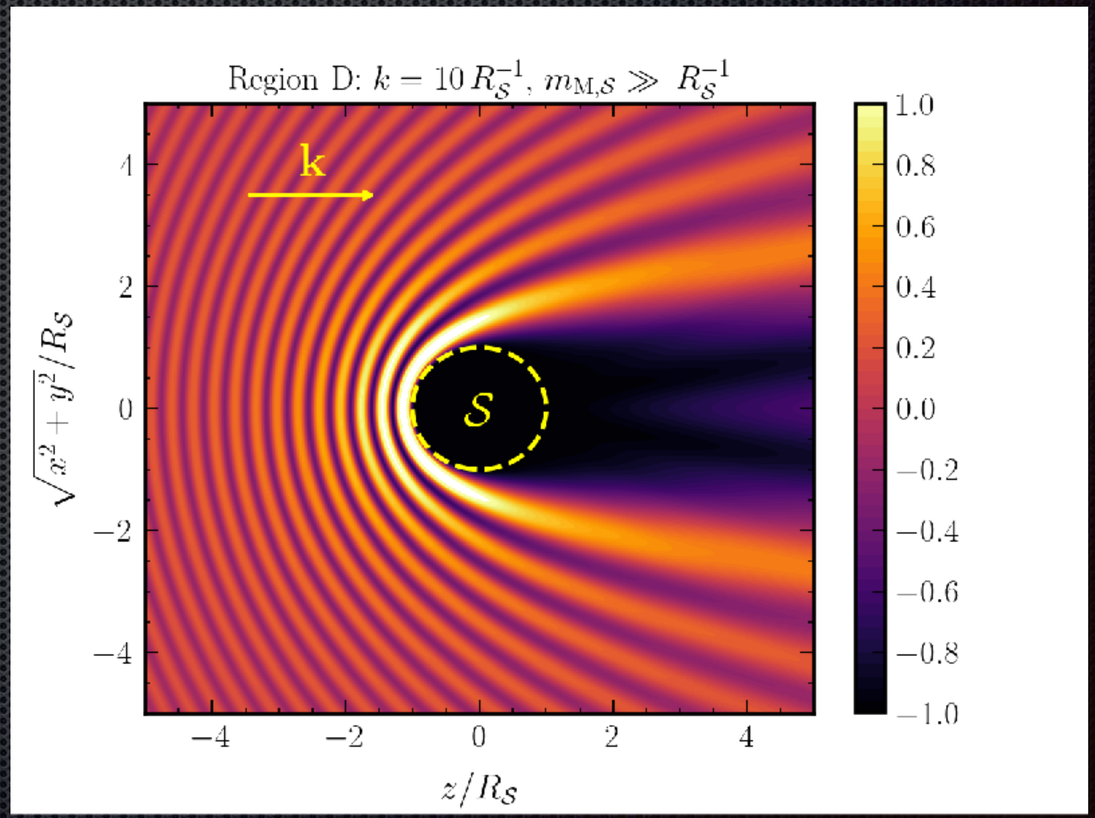

Classification

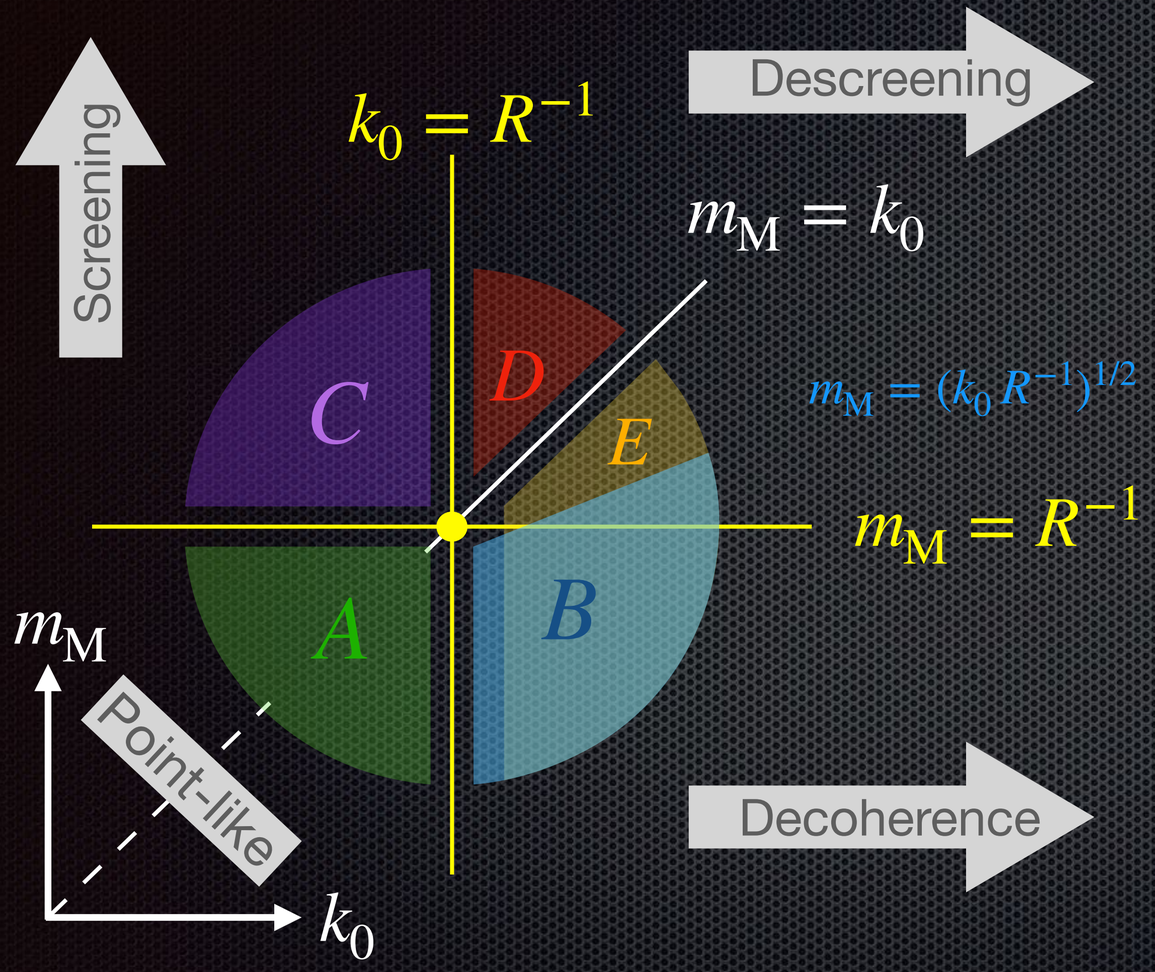

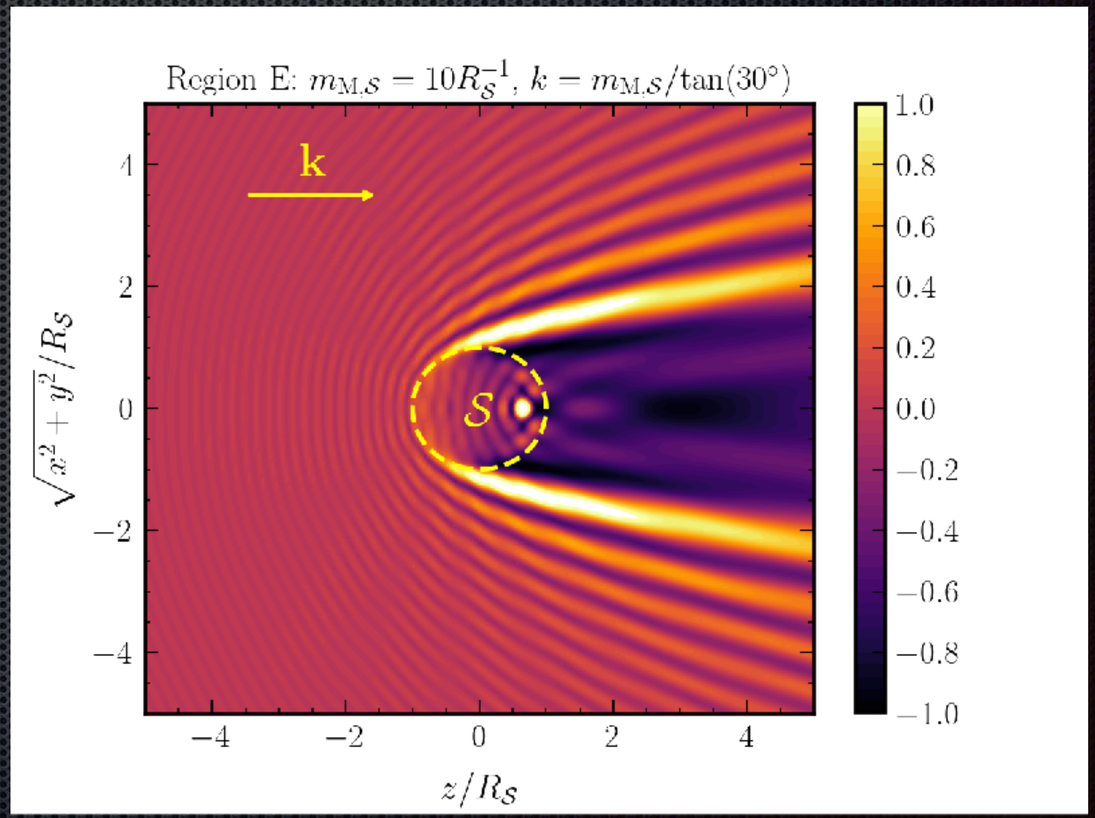

Scattering Force

$$F_{\rm sc} \sim \frac{(m_{\rm M}^2 V_R)^2}{4\pi} \rho_\phi v_\phi^2 \times \mathscr{F}_{sc}$$

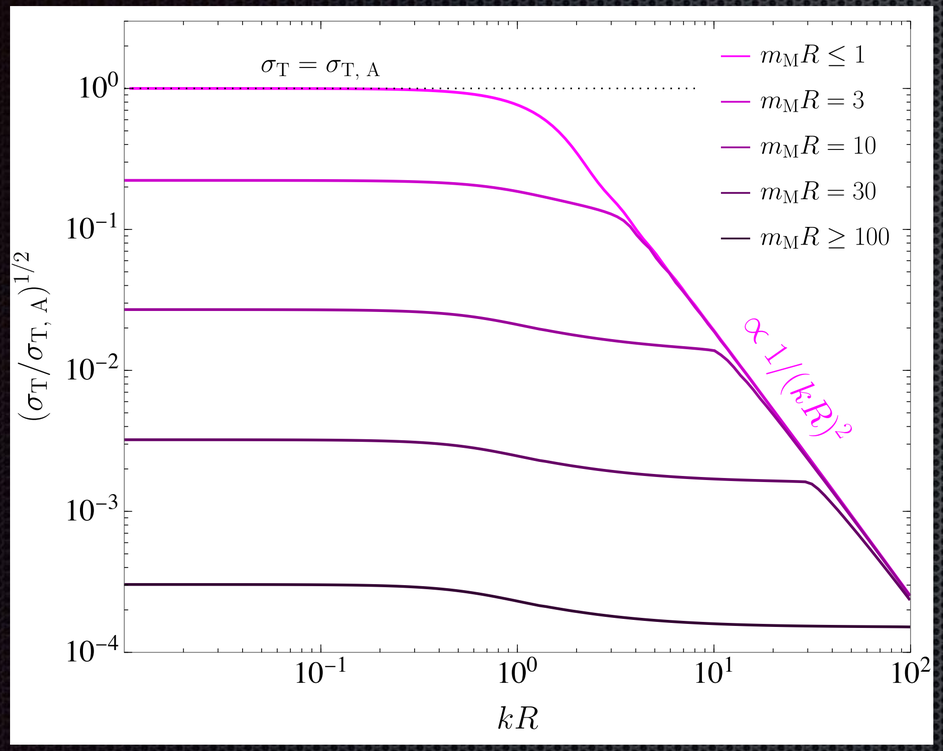

$\mathscr{F}_{\rm sc}$

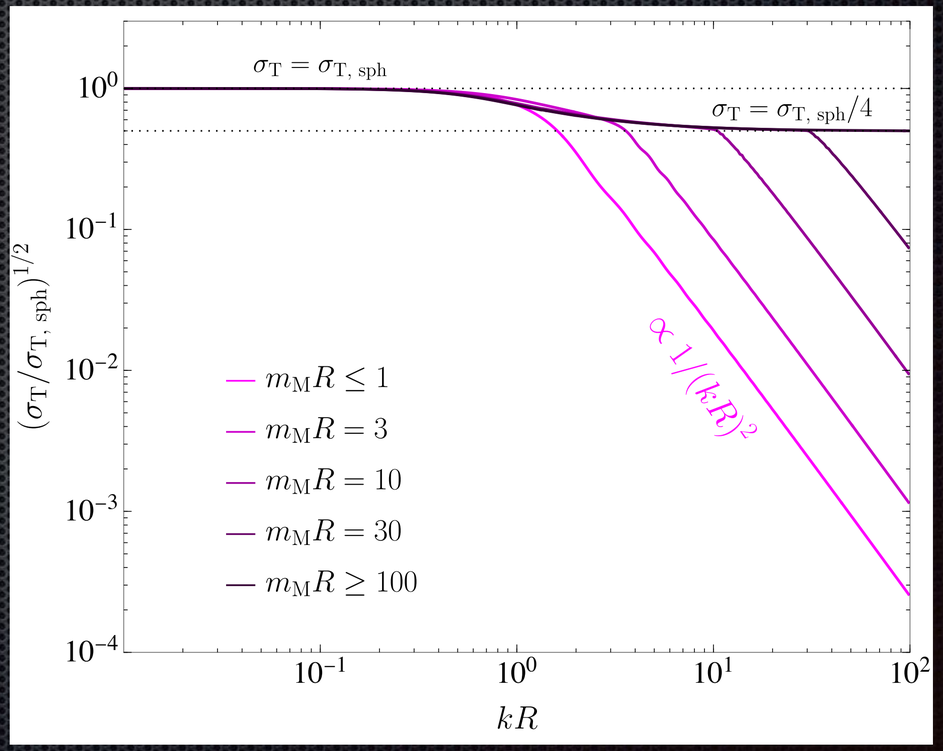

$\mathscr{F}_{\rm sc}/\mathscr{F}_{\rm sph}$

Scattering Force

$$F_{\rm sc} \sim \frac{(m_{\rm M}^2 V_R)^2}{4\pi} \rho_\phi v_\phi^2 \times \mathscr{F}_{sc}$$

Descreening vs Decoherence

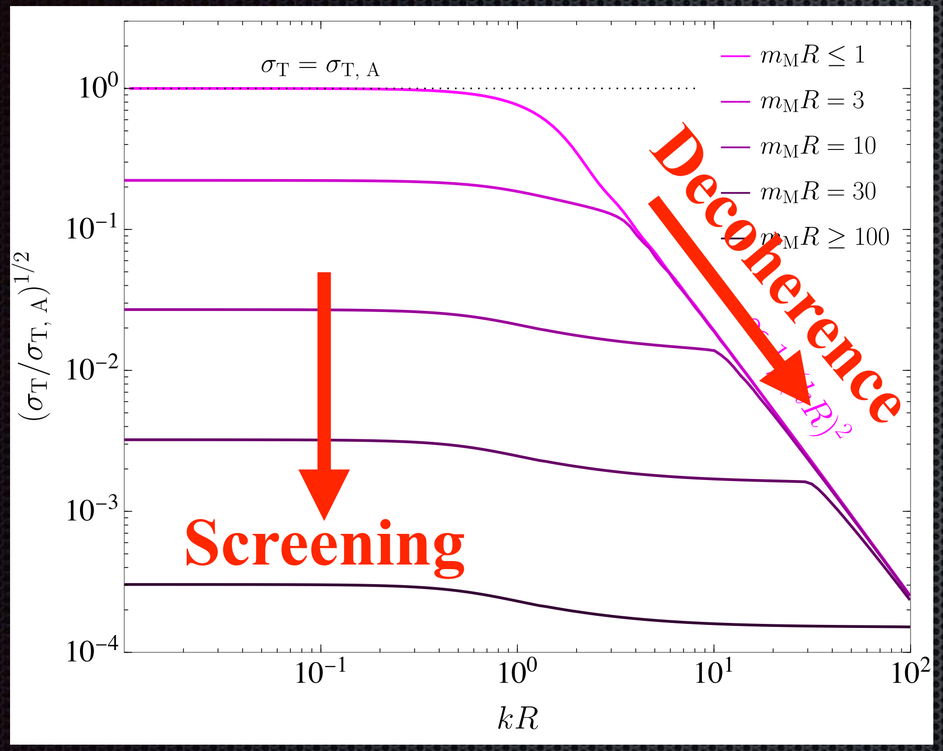

$\mathscr{F}_{\rm sc}$

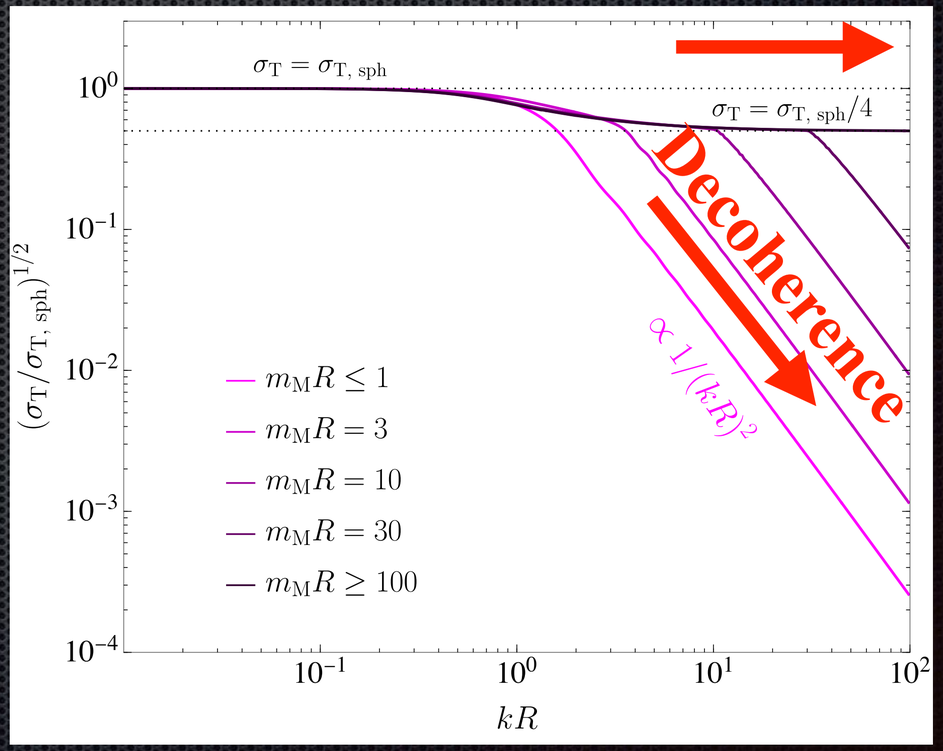

$\mathscr{F}_{\rm sc}/\mathscr{F}_{\rm sph}$

Background-Induced Force: Perturbative

$$V_{\rm bg} \sim \frac{\rho_\phi}{m_\phi^2}\,(m^2_{{\rm M},\mathcal{S}} V_{R,\mathcal{S}})(m^2_{{\rm M},\mathcal{T}} V_{R,\mathcal{T}})\,\frac{1}{r} \times \mathscr{F}$$

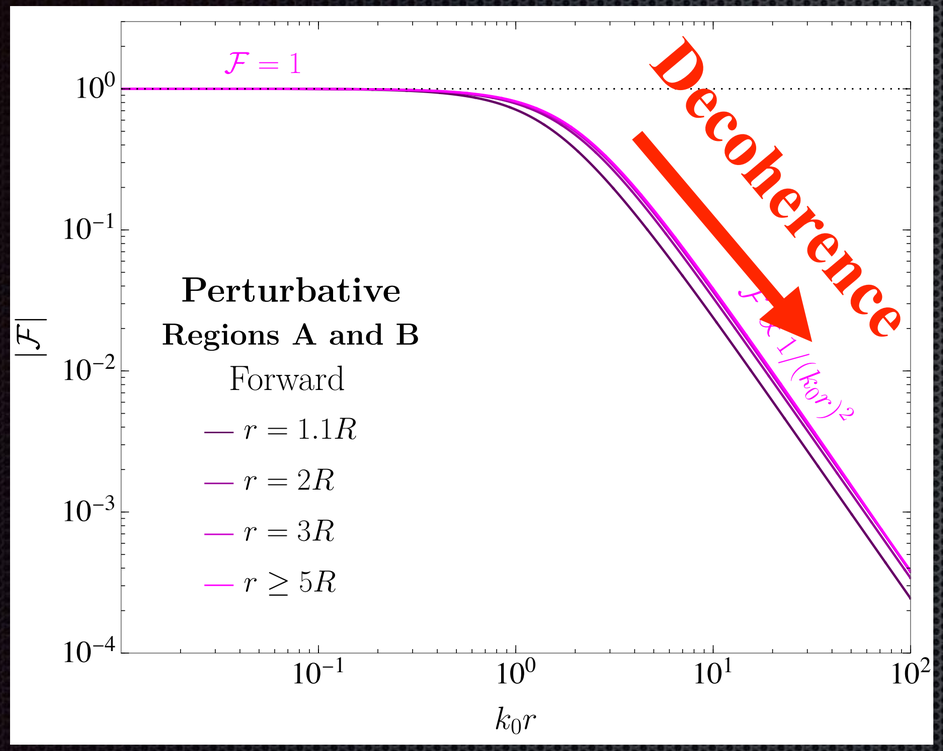

Forward Direction

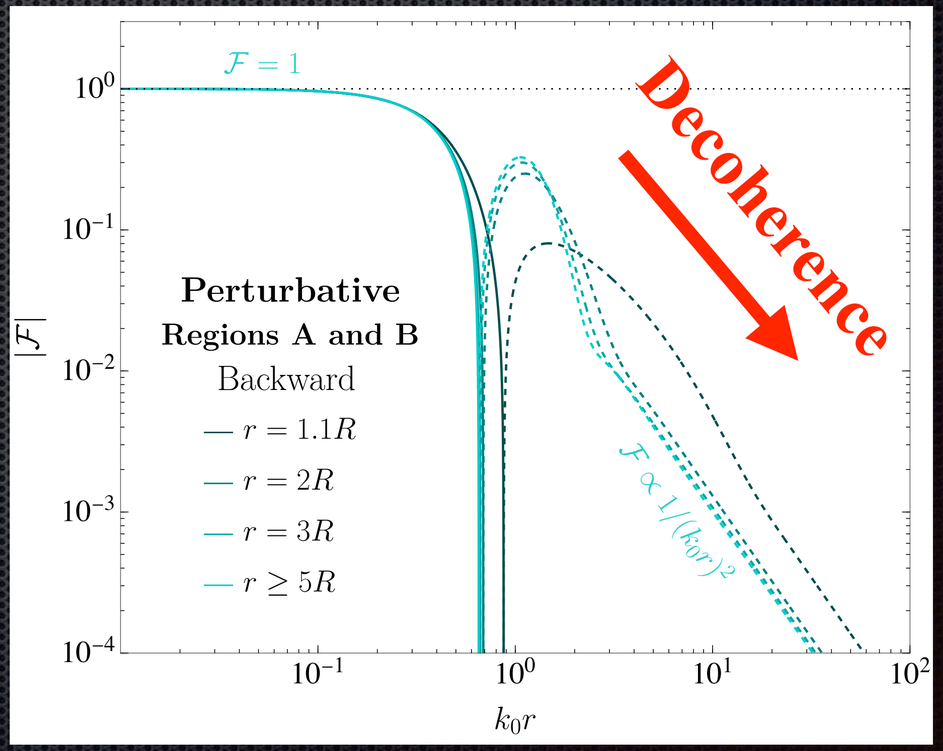

Backward Direction

Background-Induced Force: Finite Barrier

$$V_{\rm bg} \sim \frac{\rho_\phi}{m_\phi^2}\,(m^2_{{\rm M},\mathcal{S}} V_{R,\mathcal{S}})(m^2_{{\rm M},\mathcal{T}} V_{R,\mathcal{T}})\,\frac{1}{r} \times \mathscr{F}_{\rm sph} \times \widetilde{\mathscr{F}} \qquad \mathscr{F}_{\rm sph} \simeq \frac{3}{(m_{\rm M} R)^2}$$

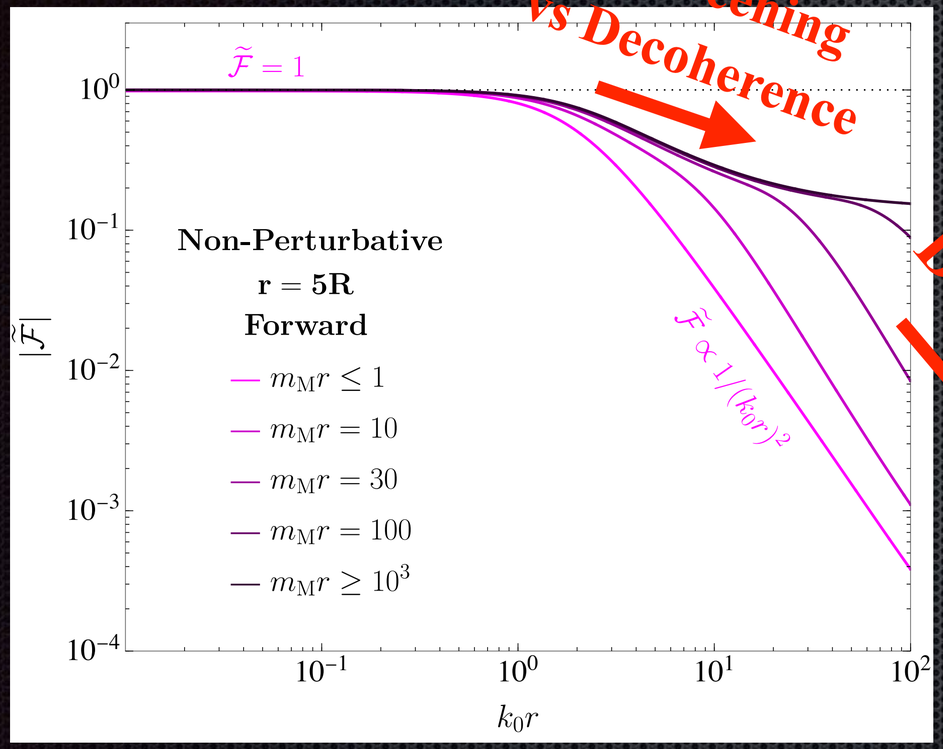

Forward Direction

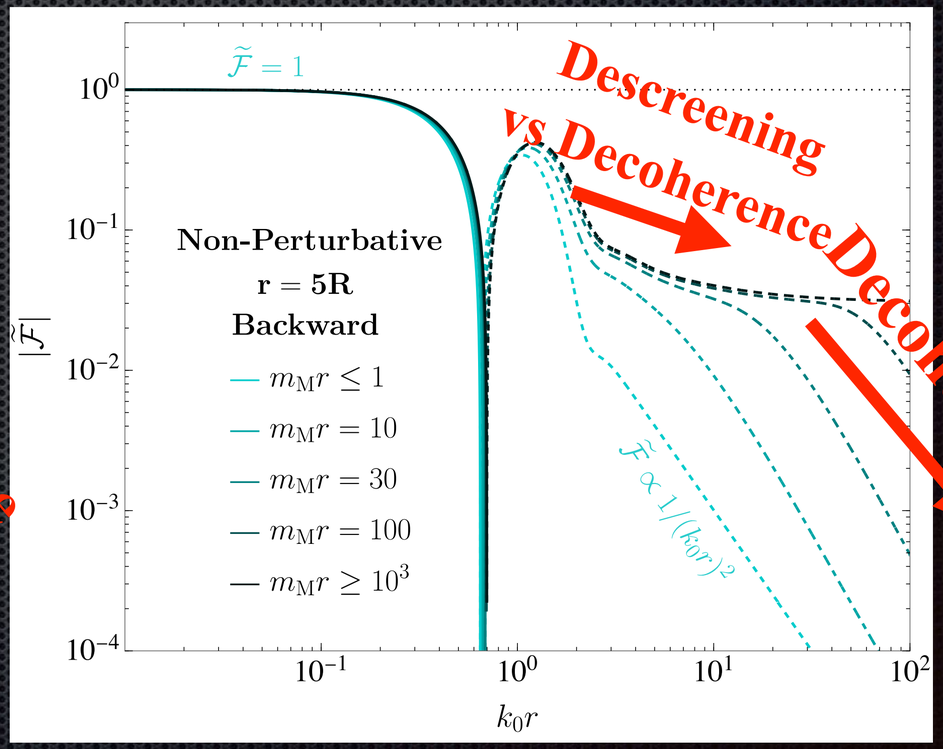

Backward Direction

Background-Induced Force: Hard Sphere

$$V_{\rm bg} \sim \frac{\rho_\phi}{m_\phi^2}\,(m^2_{{\rm M},\mathcal{S}} V_{R,\mathcal{S}})(m^2_{{\rm M},\mathcal{T}} V_{R,\mathcal{T}})\,\frac{1}{r} \times \mathscr{F}_{\rm sph} \times \widetilde{\mathscr{F}} \qquad \mathscr{F}_{\rm sph} \simeq \frac{3}{(m_{\rm M} R)^2}$$

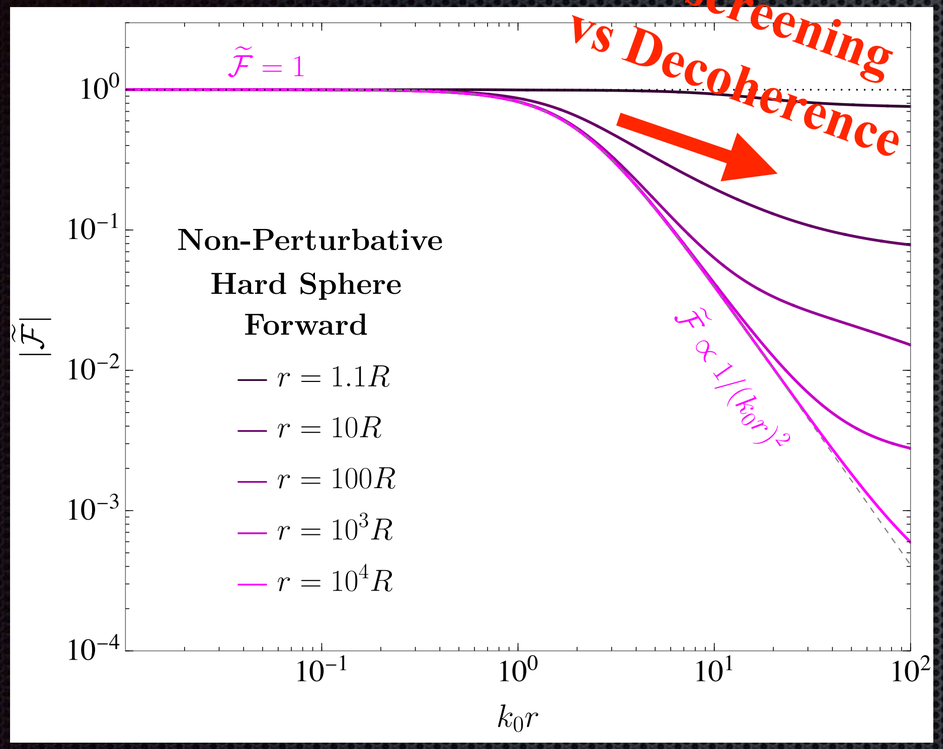

Forward Direction

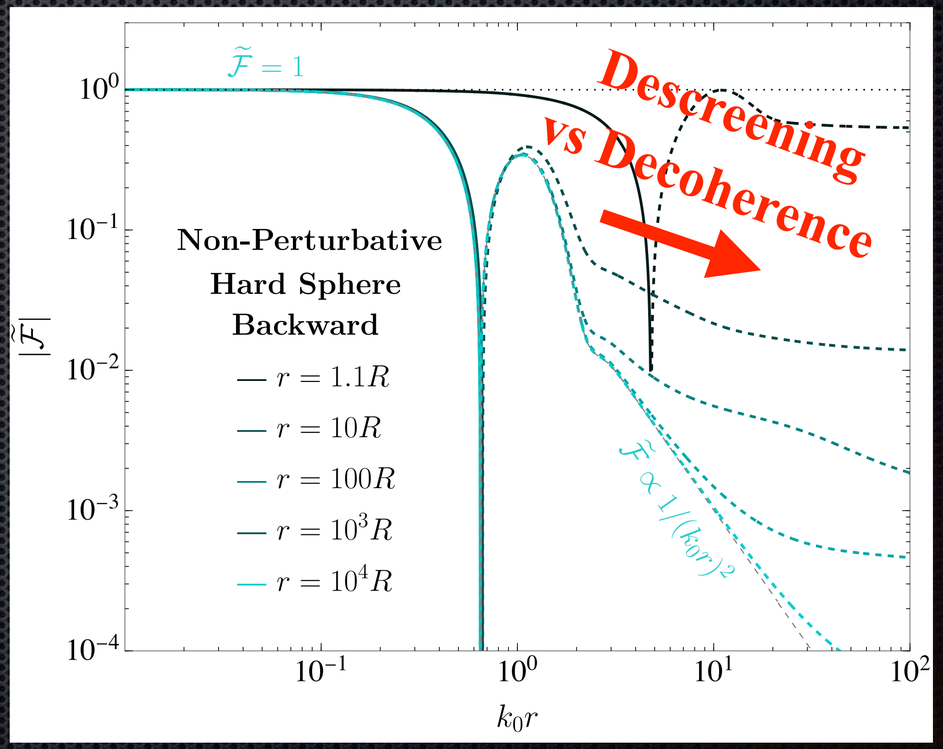

Backward Direction

Experimental Sensitivity

Experiments	Acceleration
MICROSCOPE	$\sim 10^{-14}\,\mathrm{m/s^2}$
Eot-Wash	$\sim 10^{-15}\,\mathrm{m/s^2}$
Galileo Galilei Satellite	$\sim 10^{-16}\,\mathrm{m/s^2}$
Deep Space Mission	$\sim 10^{-18}\,\mathrm{m/s^2}$

Test Mass : $R \sim 1\,\mathrm{cm} - 10\,\mathrm{cm}$

Experimental Sensitivity

Experiments	Acceleration
MICROSCOPE	$\sim 10^{-14}\,\mathrm{m/s^2}$
Eot-Wash	$\sim 10^{-15}\,\mathrm{m/s^2}$
Galileo Galilei Satellite	$\sim 10^{-16}\,\mathrm{m/s^2}$
Deep Space Mission	$\sim 10^{-18}\,\mathrm{m/s^2}$
$T \sim 10\,\mathrm{K}, \quad Q \sim 10^8$	$\sim 10^{-20}\,\mathrm{m/s^2}$
SQL, $\quad Q \sim 10^8$	$\sim 10^{-27}\,\mathrm{m/s^2}$

$f_{\mathrm{osc}} \sim 1\,\mathrm{mHz}$, $t_{\mathrm{int}} \sim 3\,\mathrm{years}$

Test Mass : $\quad R \sim 1\mathrm{cm} - 10\,\mathrm{cm}$

Experimental Sensitivity

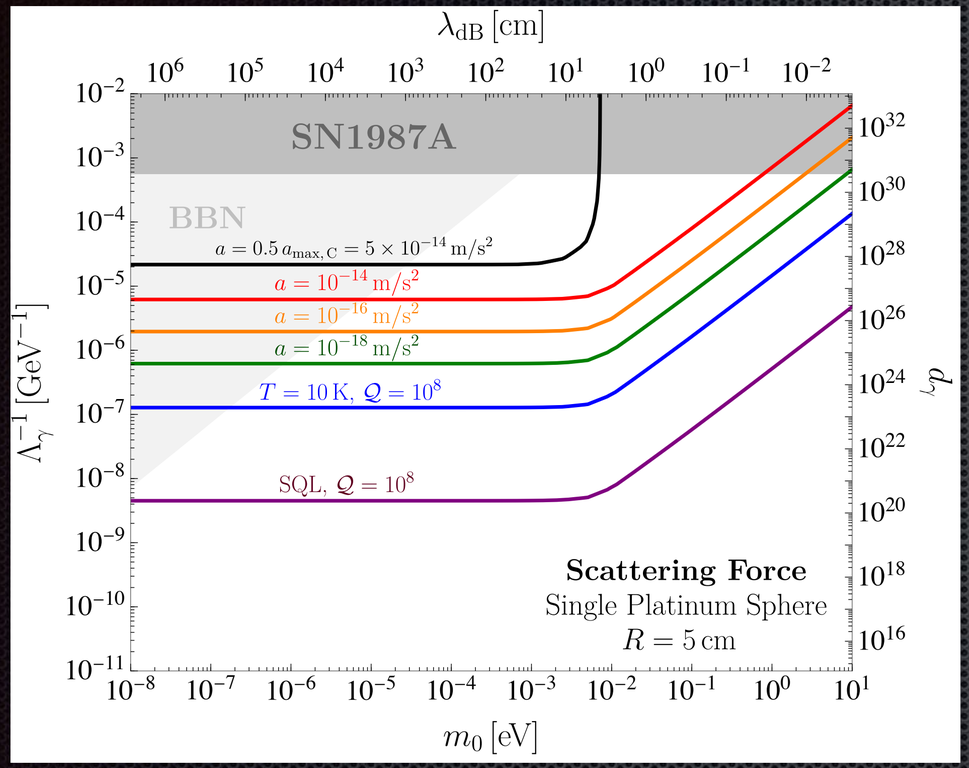

Scattering Force

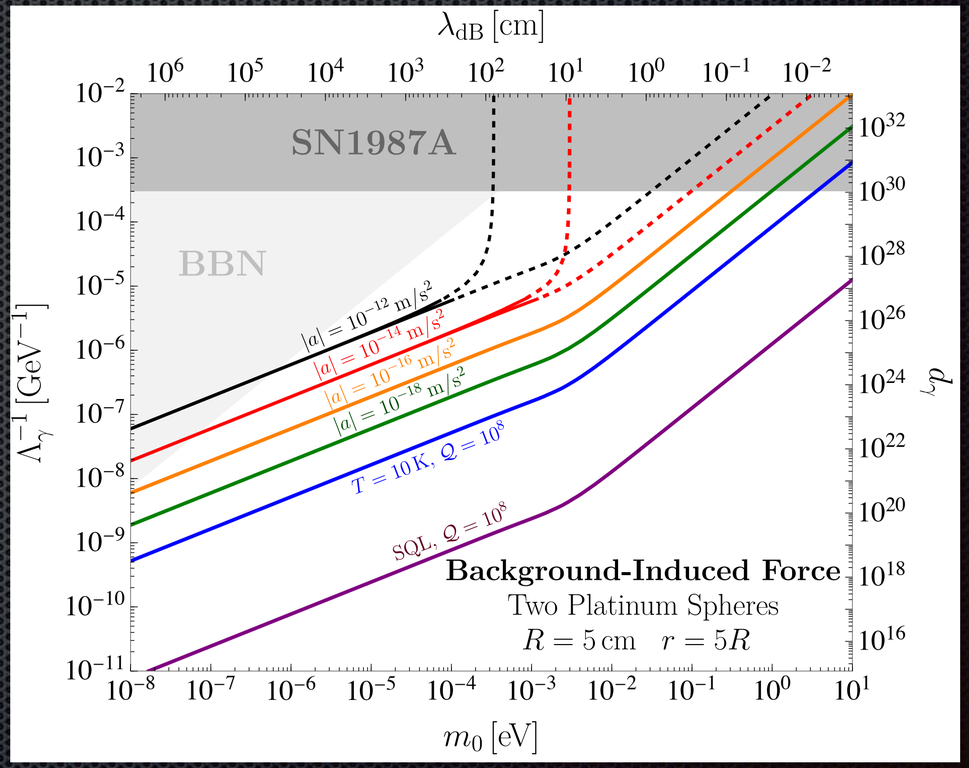

Background-Induced Force

MICROSCOPE Satellite

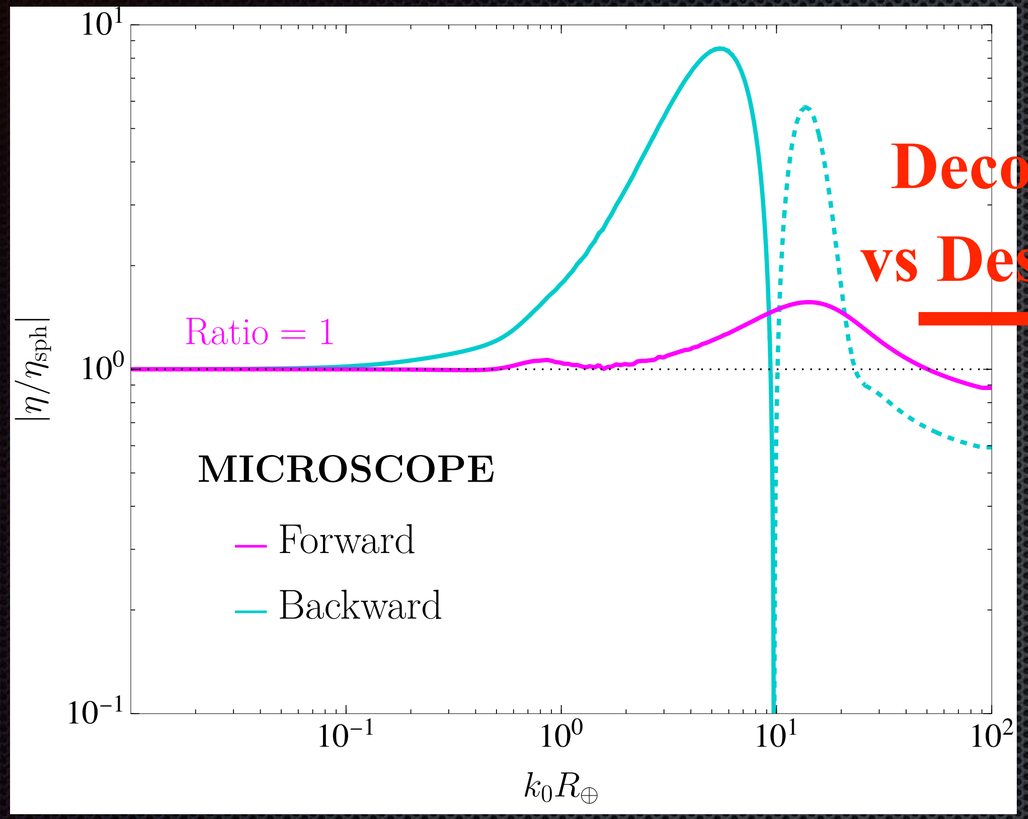

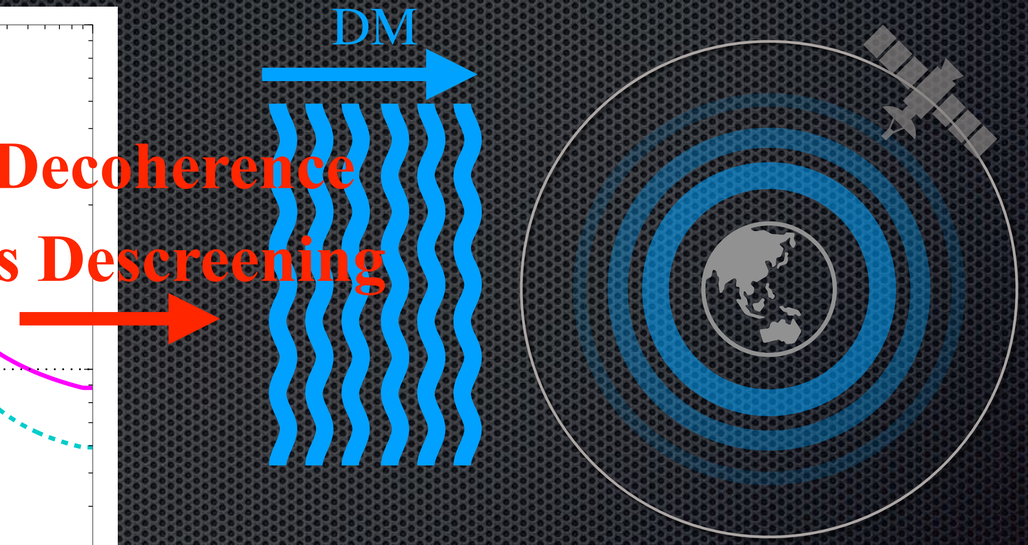

1. $\mathcal{O}(10)$ Difference
2. $m > 10^{-8}$eV,
Non-centripetal Force

MICROSCOPE Satellite

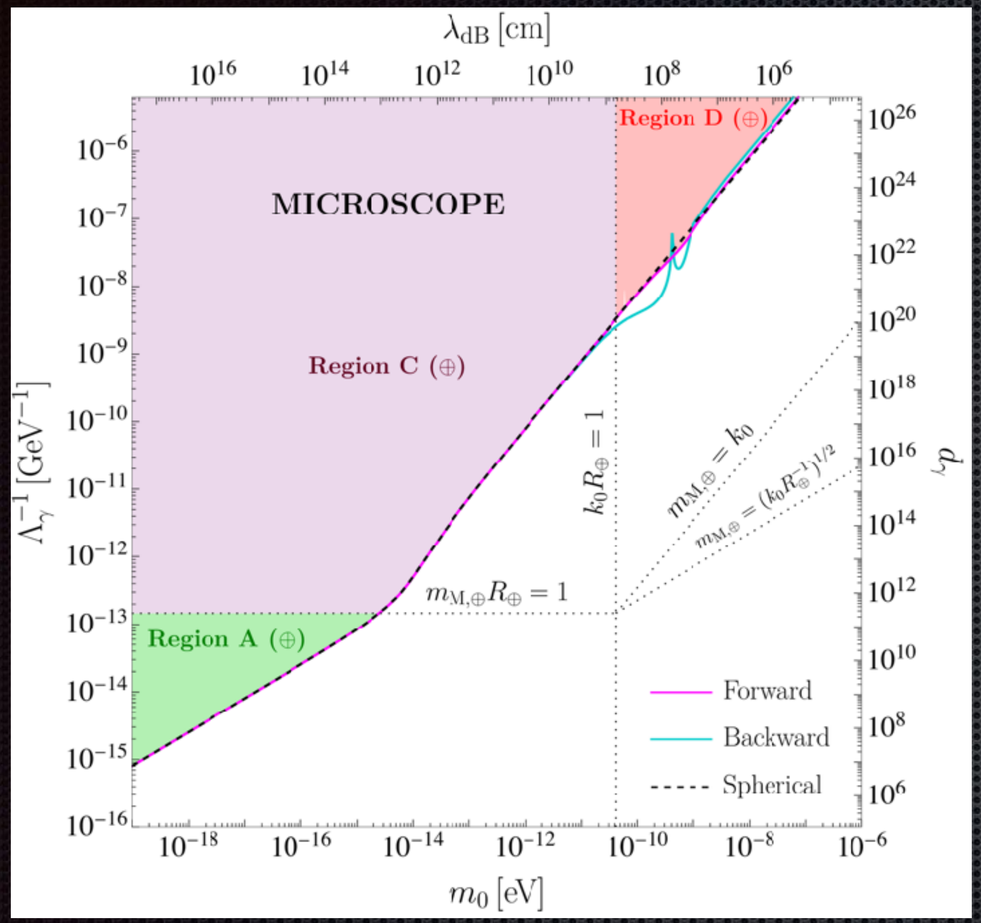

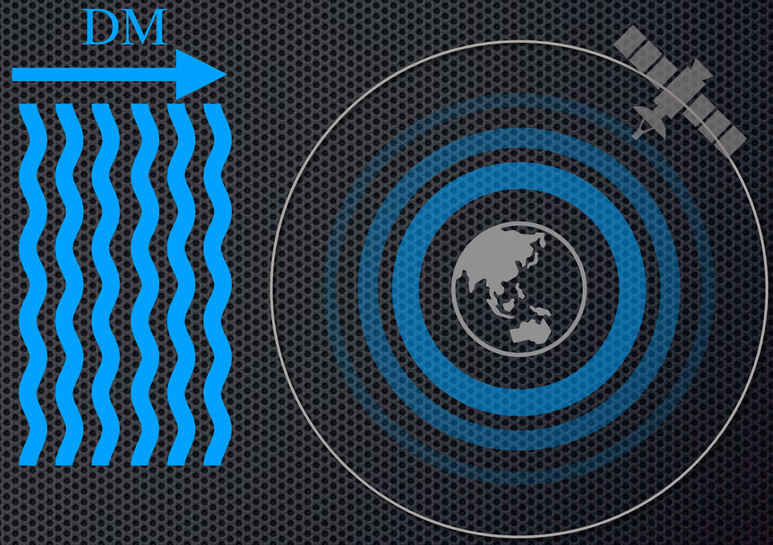

$$\eta = \frac{|\mathbf{a}_A - \mathbf{a}_B|}{|\mathbf{a}_A + \mathbf{a}_B|} \sim 10^{-14}$$

Conclusions

1. The quadratic coupling arises in dilaton, axion, and other scalar models.

2. Quadratic couplings can be probed via matter effects, which manifest as a scattering force and a background-induced force. Both forces produce accelerations of test masses that can be measured using precision accelerometers.

3. Previous studies were limited to specific regions of the parameter space. By employing partial wave analysis, we develop a unified framework that covers the entire parameter space, including both perturbative and non-perturbative regimes. We highlight three effects: the decoherence effect, the screening effect, and the descreening effect.

4. We discuss the sensitivities for the accelerometer experiments, which detects the acceleration induced by the scattering force and background-induced force.

5. We also revisited the MICROSCOPE equivalence principle test and extend the constraints to the high-momentum regime $kR_\oplus \gg 1$.

Appendix

Partial Wave + Phase Space

$$\psi_{\rm tot} = \psi_{\rm in} + \psi_{\rm sc}$$

$$\begin{cases} \psi_{\rm in} = |\phi_0|\, e^{i\mathbf{k}\cdot\mathbf{r}} \\ \psi_{\rm sc} = \sum_{l=1}^{l_{\rm max}} \psi_{{\rm sc},l} \end{cases}$$

$$l_{\rm max} \sim kR \leq 10^4$$

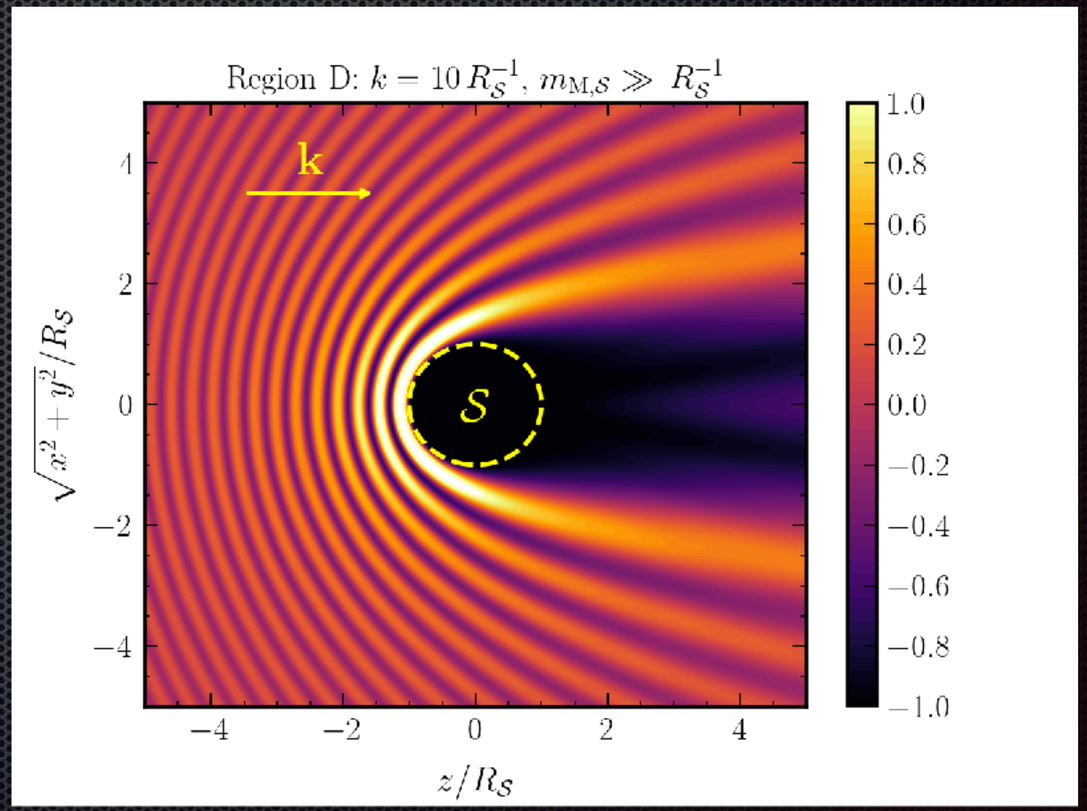

Partial Wave + Phase Space

$$V_{\rm bg}(\mathbf{k}) \propto |\psi_{\rm tot}(\mathbf{k})|^2$$

$$\langle V_{\rm bg}\rangle_{\mathbf{k}} = \frac{1}{n_\phi}\int_{\mathbf{k}} f_\phi(\mathbf{k}) V_{\rm bg}(\mathbf{k})$$

$$f_\phi(\mathbf{k}) = n_\phi \left(\frac{2\pi}{\sigma_k^2}\right)^{3/2} \exp\left[-\frac{(\mathbf{k}-\mathbf{k}_0)^2}{2\sigma_k^2}\right]$$

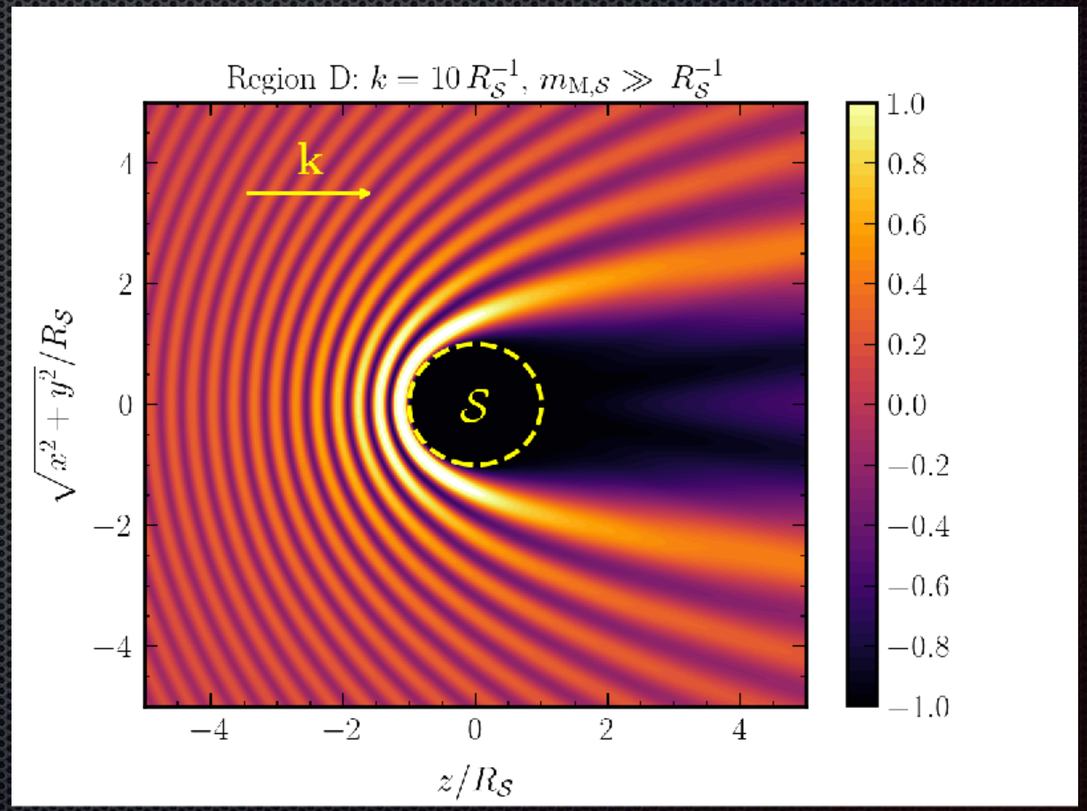

Descreening Effect

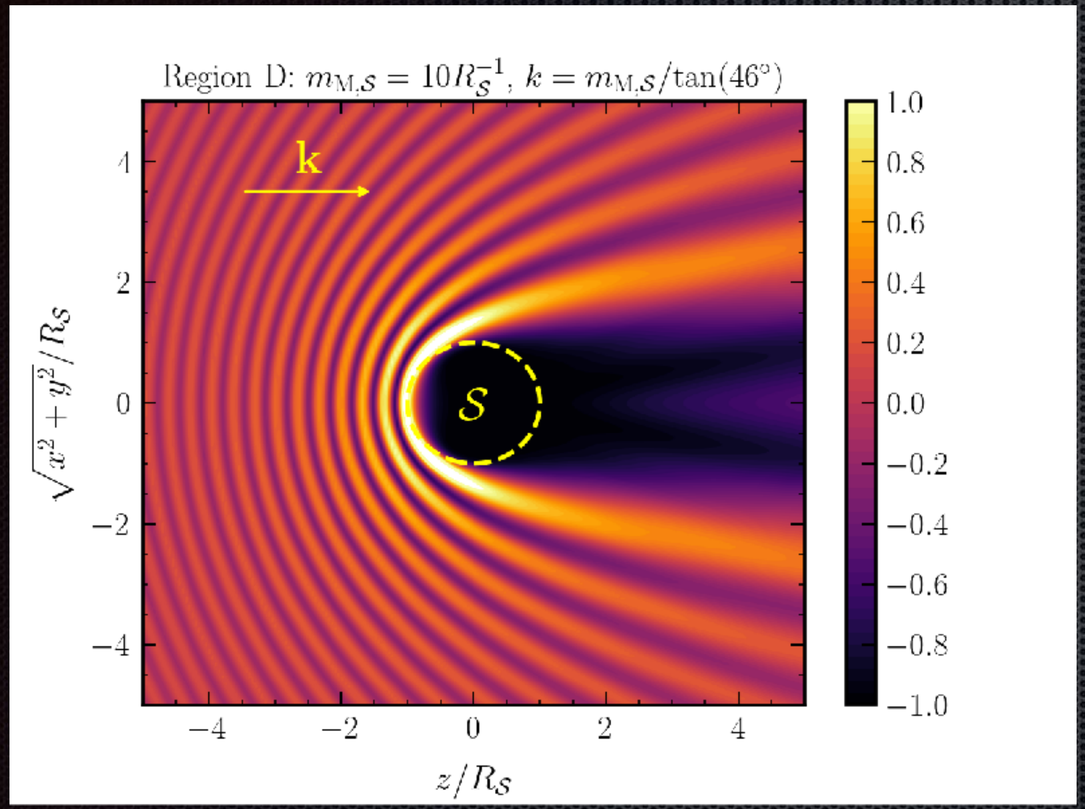

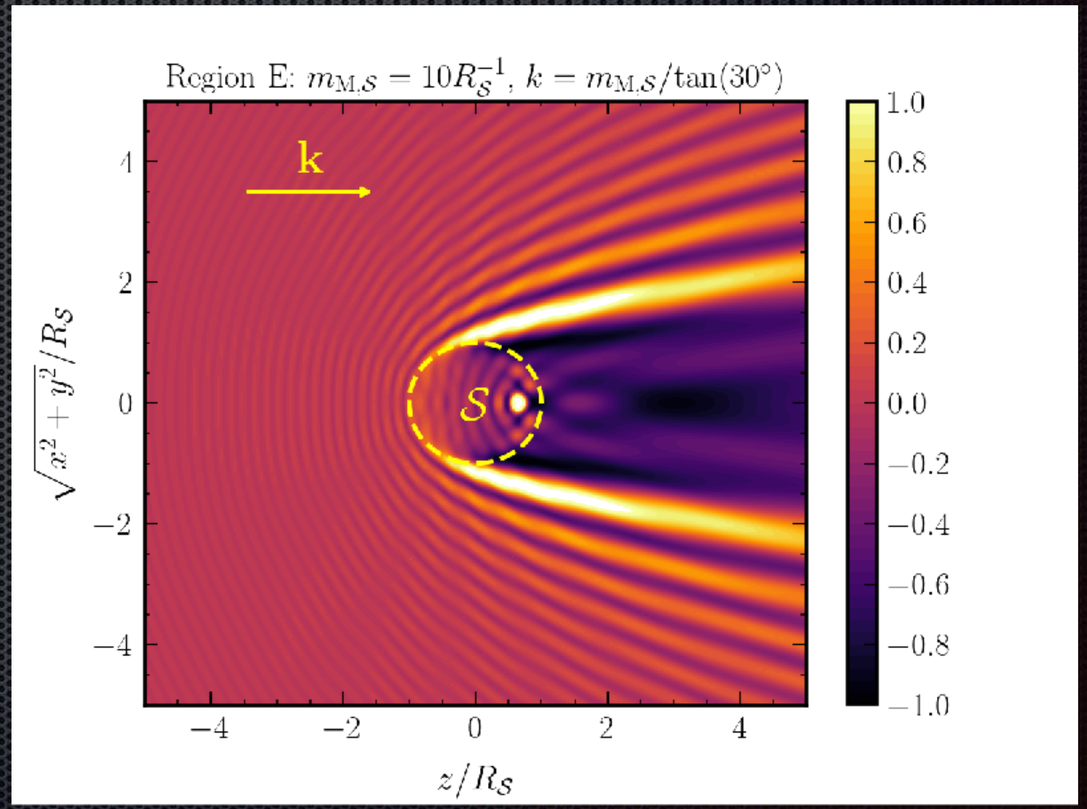

Descreening Effect

$$V_{\rm bg} \sim \frac{\rho_\phi}{m_\phi^2}\,(m_{\rm M}^2 V_R)^2\,\frac{1}{r} \times \mathscr{F}_{\rm sph} \times \widetilde{\mathscr{F}}$$

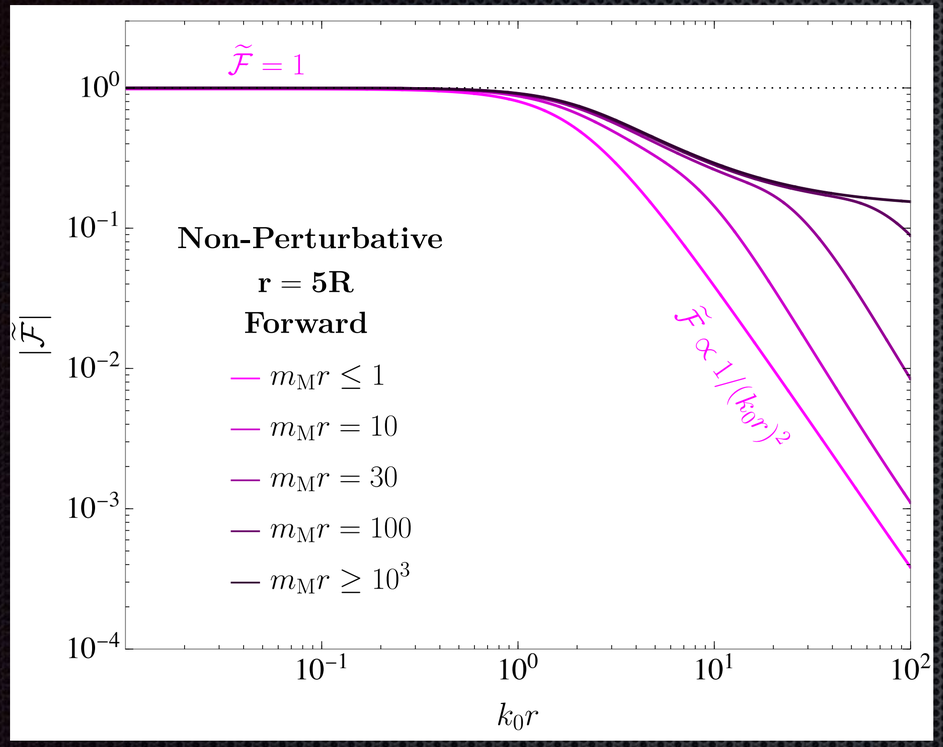

Forward Direction

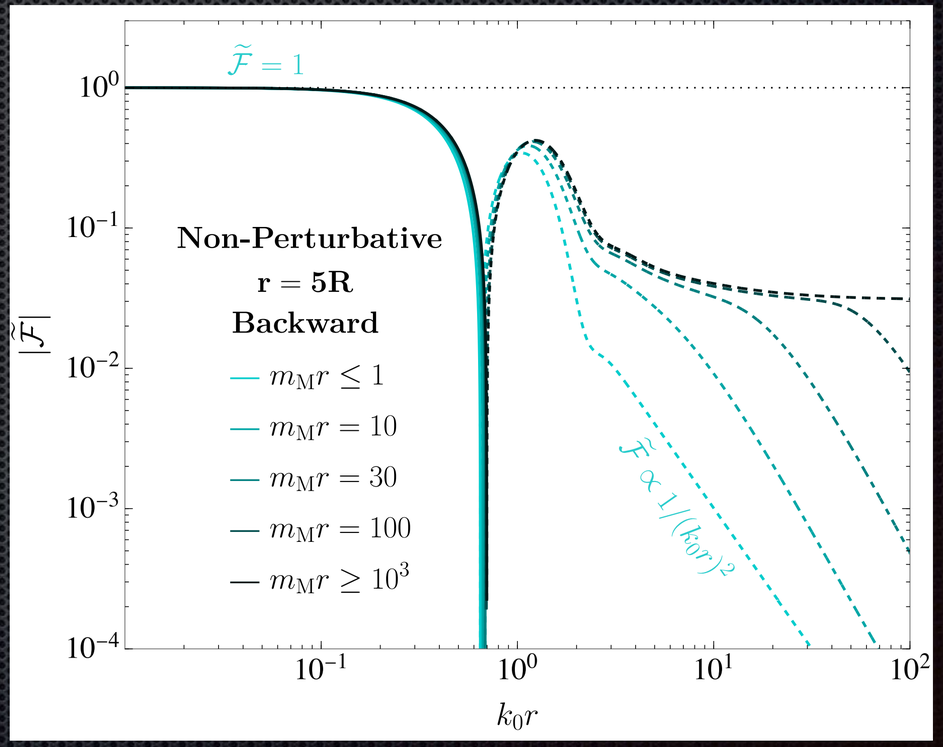

Backward Direction

Spherical Symmetric Ansatz

$$\nabla^2 \psi_{\rm sph} = m_{\rm M}^2\, \theta(R-r)\, \psi_{\rm sph}$$

$$\psi_{\rm sph} = |\phi_0| \left[1 - \frac{m_{\rm M} R - \tanh(m_{\rm M} R)}{m_{\rm M} r}\right] \simeq \min\left[1, \frac{3}{(m_{\rm M} R)^2}\right]$$

Screening Effect

Hees, et al, 2018,
Banerjee, et al., 2022

Classification of $\mathbf{F}_{\mathrm{bg}}$

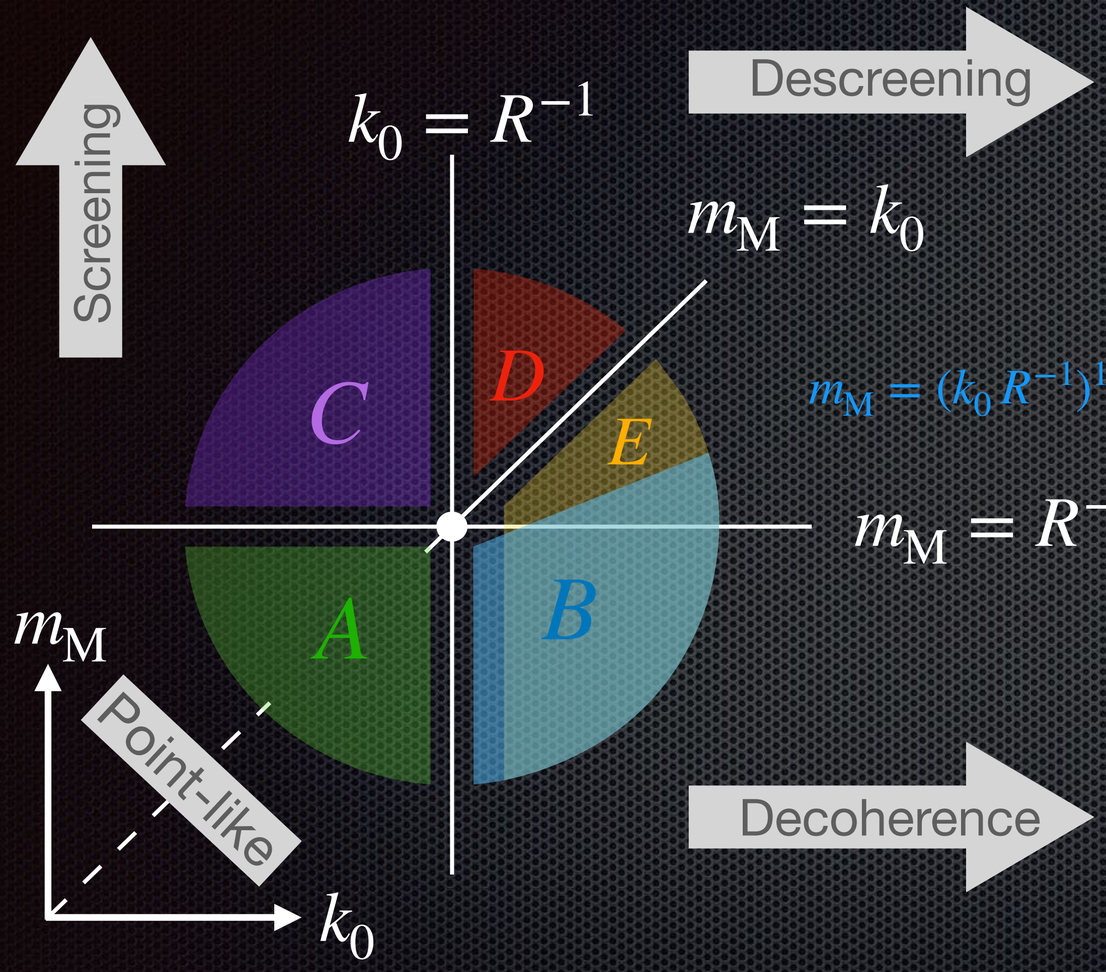

★ Region: A

Ferrer, Grifols, 2001,
Barbosa, Fichet, 2024…

★ Regions: A+B

Van Tilburg, 2024

★ Regions: A+C

Hees, et al, 2018,
Banerjee, et al., 2022

Our work

A+B+C

+D+E